Review

Gels that Serve as Mucus Simulants: A Review

Appu Vinod , Rafael Tadmor * , David Katoshevski , Ephraim Gutmark

Posted Date: 2 June 2023

doi: 10.20944/preprints202306.0172.v1

Keywords: Mucus; synthetic hydrogels; polymers; gel networks

 doi:10.20944/preprints202306.0172.v1

Review

Gels That Serve as Mucus Simulants: A Review

Appu Vinod [1], Rafael Tadmor [1,*], David Katoshevski [2] and E. J. Gutmark [3]

[1] Ben Gurion University, Department of Mechanical Engineering, Beer Sheva, Israel; appu@post.bgu.ac.il
[2] Ben Gurion University, Department of Civil and Environmental Engineering, Beer Sheva, Israel; davidk@bgu.ac.il
[3] Aerospace Engineering & Engineering Mechanics, University of Cincinnati, Cincinnati, OH; gutmarej@ucmail.uc.edu
* Correspondence: tadmorr@bgu.ac.il

Abstract: Mucus is a critical part of the human body's immune system which traps and carries away various particulates such as anthropogenic pollutants, pollen, viruses etc. Various synthetic hydrogels have been developed to mimic mucus, using different polymers as their backbones. Common to these simulants is a three-dimensional gel network which is physically crosslinked and is capable of loosely entrapping water within. Two of the challenges in mimicking mucus using synthetic hydrogels include the need to mimic the rheological properties of the mucus and its ability to capture particulates (its adhesion mechanism). In this paper, we review the existing mucus simulants and discuss their rheological, adhesive and tribological properties. We show that most, but not all, simulants indeed mimic the rheological properties of the mucus but only one mimics the ability of mucus to capture particulates.

Keywords: Mucus; synthetic hydrogels; polymers; gel networks

Introduction

Mucus is a viscoelastic fluid produced by the epithelial secretory cells in the mucous membrane [1]. In the tracheobronchial tract, it serves (among other functions) to protect from foreign agents that may enter the human body, as well as hydrates these cells by forming a coating over them [2–5]. In various conditions such as COPD, asthma, COVID 19, mucus may accumulate in the lungs and several techniques have been suggested to clear the mucus out of the lungs.

The adhesivity of mucus mimicking gels have been particularly useful for facilitating a localized drug delivery [6]. The localized drug delivery is achieved either by retaining a large amount of the drug at one specific location in or by providing a specific quantity of drug to one specific location on a regular interval [6]. To design such devices, there is an interest to understand the rheological and the tribological properties of mucus.

Here, in this review, we take into consideration different gel compositions that mimic human mucus and their tribological and rheological properties.

1. Native Human Mucus

Human airway mucus is primarily composed of 97% of water, 3.0 % of solids [7]. These solids consist of anionic glycoproteins, and mucin, which give mucus its hydrogel-like nature.

a) Collection of Native Human Mucus

Obtaining native mucus in large quantity for conducting several experiments can be challenging [8]. The main challenge lies in finding the right method for its collection. One method involves using a bronchoscopy brush to collect mucus from the human airway [9–13]. However, introducing a bronchoscopy brush into the airway mucus presents two major bottlenecks: (i) only a small volume of mucus can be collected this way, and (ii) it is difficult to obtain mucus from the

 doi:10.20944/preprints202306.0172.v1

airway without causing any physical damage due to the introduction of the bronchoscopy brush [2]. Despite these challenges, the bronchoscopy technique allows for the collection of mucus from a controlled area without salivary contamination. It is important to note that due to the difficulties mentioned earlier in collecting mucus from the human airway, most of the rheological and tribological studies of mucus are conducted using sputum samples [2].

b) Rheological Properties of Human Mucus

Rheological properties play a crucial role in characterizing both natural mucus and its synthetic versions. Before delving into the rheological studies, let us focus on two properties: (i) storage (G′) and (ii) loss moduli (G″). Together, these properties determine the bulk rheology of mucus. The storage modulus reflects the ability of macromolecules to store energy through bending and rotation of the bonds within and between the molecules that constitute the mucus. On the other hand, the loss modulus represents the amount of energy lost as the macromolecules move within the solvent.

The unique biophysical properties of mucus are linked to its mucin concentration, which can significantly impact its biophysical and transport properties even with slight changes [14]. High molecular weight mucin molecules contribute to the characteristic viscoelastic properties of human mucus [14].

Theoretical analyses and experiments have been developed to study the relationship between G′ and G″ and the applied shear, which helps to determine whether the system behaves like a gel or a solution. The relation of G′ and G″ with shear frequency (ω) is given by Equation (1):

$$G' = \frac{G''}{\tan\left(\frac{n\pi}{2}\right)} = \frac{\pi}{\Gamma(n)\sin\left(\frac{n\pi}{2}\right)} S \quad (1)$$

Equation (1) can be re written as an inequality below:

$$G'(\omega) \sim \omega^{n'} \text{ and } G''(\omega) \sim \omega^{n''} \quad (2)$$

Here, n′ and n″ are the exponents of storage and loss modulus, respectively [15,16]. At the sol-gel transition point, n′= n″ = n, as described in the references [15,17]. The exponent n is determined by the strength of the interaction between the polymer chain segments [18,19].

Wolf et al. [20] characterized the physical properties of human native mucus based on its storage and loss moduli. Figure 1 illustrates that the storage modulus of native human mucus is greater than its loss modulus, indicating its gel-like nature. Additionally, the moduli plateaus as the angular frequency increases. This occurs because the macromolecules that compose the mucus become entangled and crosslinked, forming structures that resist deformation.

Preprints.org (www.preprints.org) | NOT PEER-REVIEWED | Posted: 2 June 2023 doi:10.20944/preprints202306.0172.v1

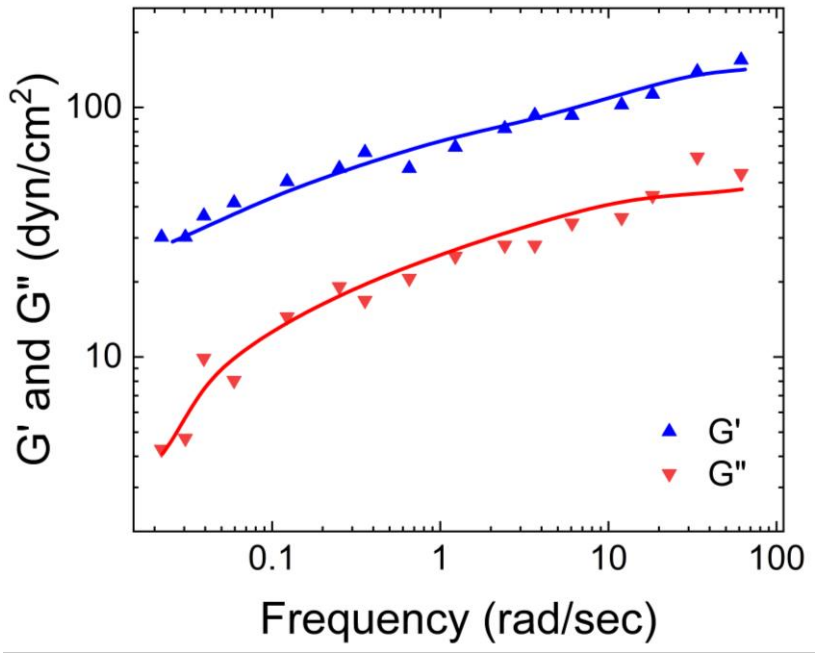

Figure 1. Storage and loss moduli versus frequency for reconstituted human cervical mucus (3.5% nondialyzable solids in 0.1 M Tris-Cl-0.055 M, NaCl, pH 7.5). (Plot reconstructed based on Figures 1 and 2 from Wolf et al. [20]).

Hill et al. [14] also characterized the rheological properties of airway mucus, including its storage and loss moduli, and viscosities over a range of shear frequencies. According to their findings shown in Figure 2, the storage modulus of human respiratory mucus was greater than its loss modulus, indicating its gel-like nature, which aligns with the observations of Wolf et al.

Furthermore, both moduli plateaued as the frequency increased. Hill et al. also measured the viscosity of human respiratory mucus and found that it ranged from 0.01 Pa. s to 60 Pa.s. The lowest viscosity was observed in mucus harvested from cell culture models, while the highest viscosity was found in mucus collected from individuals with cystic fibrosis [21].

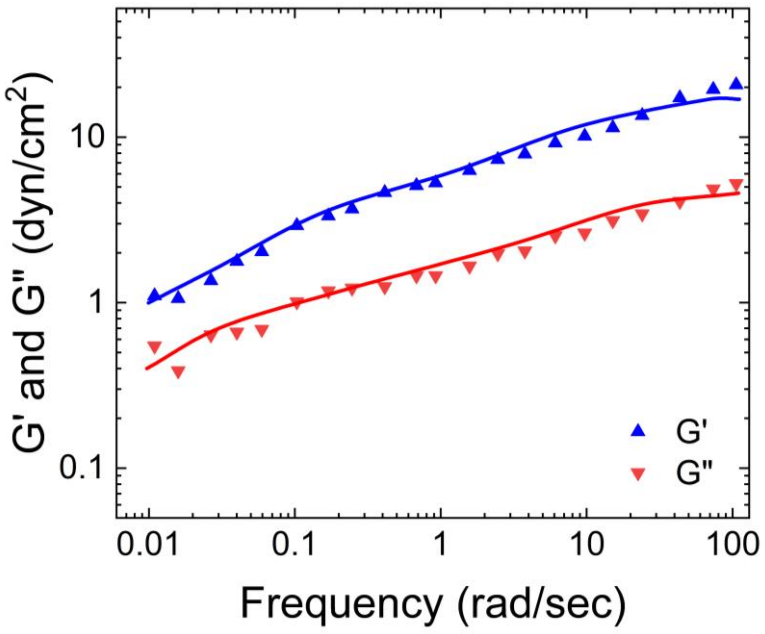

Figure 2. Storage and loss moduli vs frequency for human bronchial epithelial mucus at 1% organic solids. (Plot reconstructed based on Figure 13 of Hill et al. [14]).

 doi:10.20944/preprints202306.0172.v1

c) Tribological Properties of Human Mucus

Moving on to the tribological properties of human mucus, native mucus is secreted into the airway and spreads over the airway epithelium, which is in contact with the cilia and the periciliary fluid layer [22]. Normally, mucus is cleared from the airway by the beating action of cilia on its surface. However, the physical properties of the mucus play a crucial role in its clearance. These properties include its viscoelasticity and its interaction with the underlying epithelium [23].

Studies by Albers et al. [23] and King et al. [24] have shown that the interfacial properties of mucus affect its transportability. When discussing transportability, work must be done to separate mucus from the epithelium interface, and this work is called the work of adhesion which is calculated using the Young-dupre equation [25], as shown in Equation (1).

$$W_{SL} = \gamma_{LV}(1 + \cos\theta) \quad (3)$$

Where, W_{SL} is the work needed to separate 1cm² of an interface between the mucus and the epithelium interface, θ is the contact angle that the mucus drop makes with the epithelium interface, and γ_{LV} is the surface tension of the mucus drop.

However, obtaining accurate information about the surface tension of mucus poses a challenge when calculating the work of adhesion. The gel-like properties of mucus make it difficult to measure its surface tension accurately. Hence, researchers have used different methods to estimate it. For example, Puchelle et al. [26] directly measured the surface tension of mucus using the du Nouy ring distraction method, considering the mucus as a liquid. In contrast, Pillai et al. [27] measured the surface tension of mucus by considering it as a solid material.

Albers et al. [28] reported the work of adhesion required to separate mucus from the airway duct using two techniques: du Nouy ring method and the contact angle method. Their findings are presented in Table 1.

Table 1. Work of adhesion calculated using two different methods of mucus samples collected from two different sources.

Mucus Samples Collected from People with:	Calculated Work of Adhesion to Separate Mucus from Airway Duct	
	Du Nouy Ring	Contact Angle (Using Equation (3))
Cystic fibrosis	140 ± 30 mN/m	160 ± 20 mN/m
Chronic bronchitis	130 ± 20 mN/m	150 ± 20 mN/m

As observed by King et al. [24], Albers et al. discovered that an increase in the work of adhesion led to a decrease in the transportability of the mucus. It's important to note that while not all the hydrogels discussed below are designed to mimic human airway mucus, they are widely used in biomedical applications due to their mucus-like physical properties.

2. Synthetic Mucus Made by Polyvinyl Alcohol

Polyvinyl alcohol (PVA) hydrogels have recently gained attention due to their [29,30] hydrophilic, biodegradable, and biocompatible properties, making them a versatile material for various biomedical applications [31]. PVA hydrogels have been employed in tissue engineering to repair and regenerate a wide range of tissues and organs, such as heart valves, corneal implants, and cartilage tissue substitutes [32]. Furthermore, PVA hydrogels hold potential as mucoadhesive and drug delivery systems.

Singh et al. [33] investigated the mucoadhesive ability of PVA hydrogel crosslinked with sterculia gum and discovered that the hydrogel exhibited strong adhesive strength with the mucous membrane. This suggests that PVA hydrogel films could effectively adhere to wound sites, offering protecting against pathogens and making them a promising candidate for drug delivery applications.

 doi:10.20944/preprints202306.0172.v1

a) Rheological Properties of Polyvinyl Alcohol Hydrogels

Krise et al. [34] measured the viscosity of PVA hydrogels using Ostwald viscometers. As shown in Figure 3, increasing the concentrations of PVA resulted in higher viscosity of the hydrogel. This trend has also been observed in other studies [35–37].

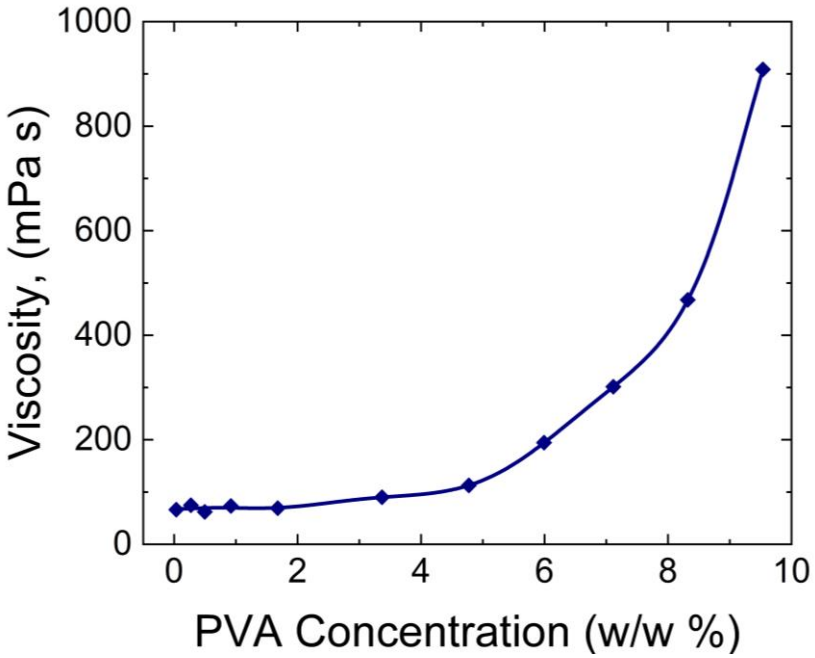

Figure 3. Plot of viscosity vs concentration of PVA hydrogel at 20°C. (Plot reconstructed based on Figure 1 from Krise et al. [34]).

Park et al. [38] used a DMA 2980 instrument to examine the variation of the storage modulus with temperature. As shown in Figure 4, by heating the sample from -20 to 260°C for both wet and dry PVA hydrogels led to a significant decrease in the storage modulus. For dry PVA, the storage modulus exhibited a steep decline until 100°C and then remained constant, after which it remained constant. On the other hand, for wet PVA, the decrease in the storage modulus was gradual until 125°C, beyond which it remained constant.

Preprints.org (www.preprints.org) | NOT PEER-REVIEWED | Posted: 2 June 2023 doi:10.20944/preprints202306.0172.v1

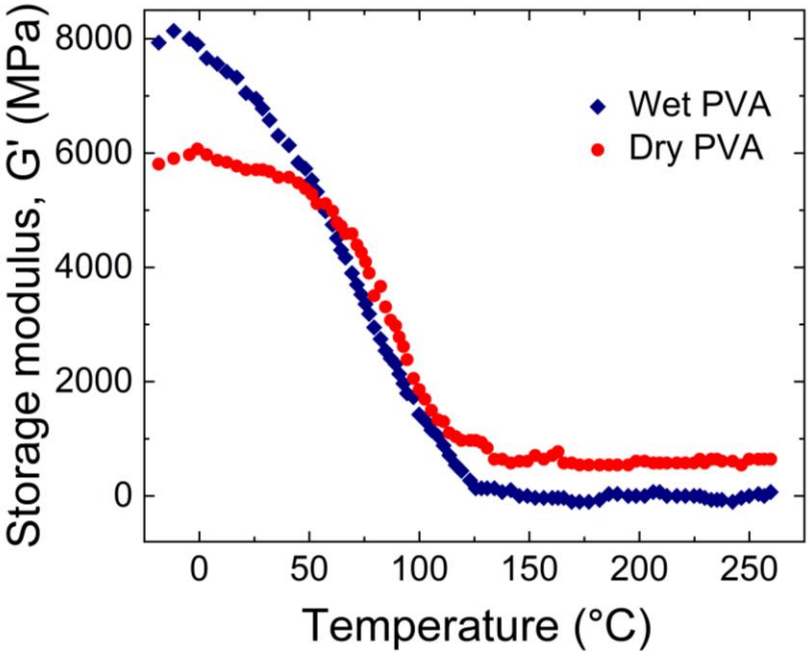

Figure 4. Storage modulus vs temperature for wet and dry PVA. The concentration of glutaraldehyde and of HCl for the preparation of PVA gel was 8.38 x 10^{-3} mol/L and 2.25 x 10^{-1} mol/L, respectively. The measurements were conducted at a 2°C/min heating rate, 1 Hz frequency. (Plot reconstructed based on Figure 5 from Park et al. [38]).

Narita et al. [39] compared the macro and micro rheology of chemically cross-linked PVA hydrogels using classic macro rheology and DWS-based micro rheology.

As shown in Figure 5, they observed that at lower frequencies, storage modulus (G′) > loss modulus (G″) for both the macro and micro rheology, whereas at higher frequencies G″ > G′ for micro rheology.

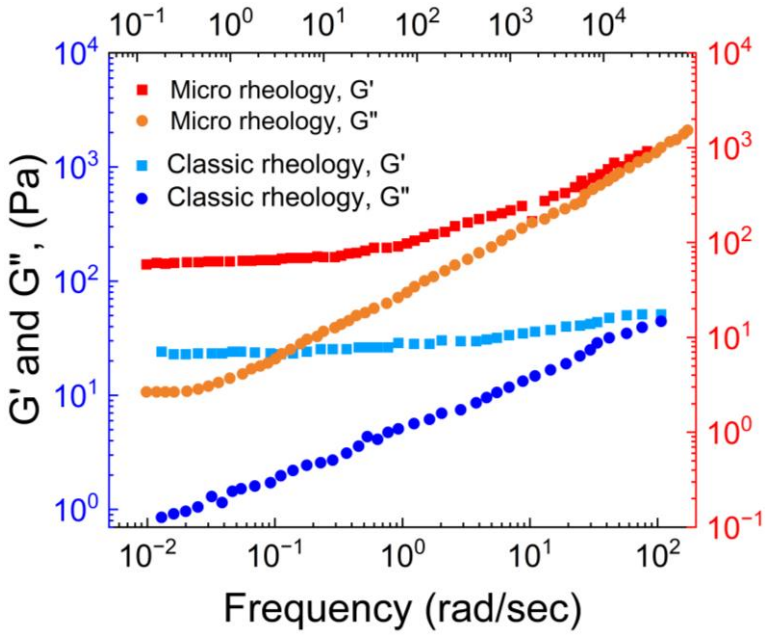

Figure 5. G′ and G″ vs frequency for a PVA hydrogel. The plots with shades of red corresponds to micro rheology, and the plots with shades of blue corresponds to macro rheology. (Plot reconstructed based on Figure 7 of Narita et al. [39]).

Preprints.org (www.preprints.org) | NOT PEER-REVIEWED | Posted: 2 June 2023 doi:10.20944/preprints202306.0172.v1

b) Tribological Properties of Poly Vinyl Alcohol Hydrogels

The tribological properties of PVA were investigated using Centrifugal Adhesion Balance [40] (CAB). CAB enabled us to measure the force required to slide a PVA hydrogel on a hydrophobic surface by manipulating the normal and lateral forces acting on the droplet [40]. In our experiment, we determined the lateral force, $f_{\parallel}$, needed to initiate the motion of a 3.0 µl poly vinyl alcohol drop (1 wt%) on a hydrophobic surface. Figure 6 illustrates the results of this experiment.

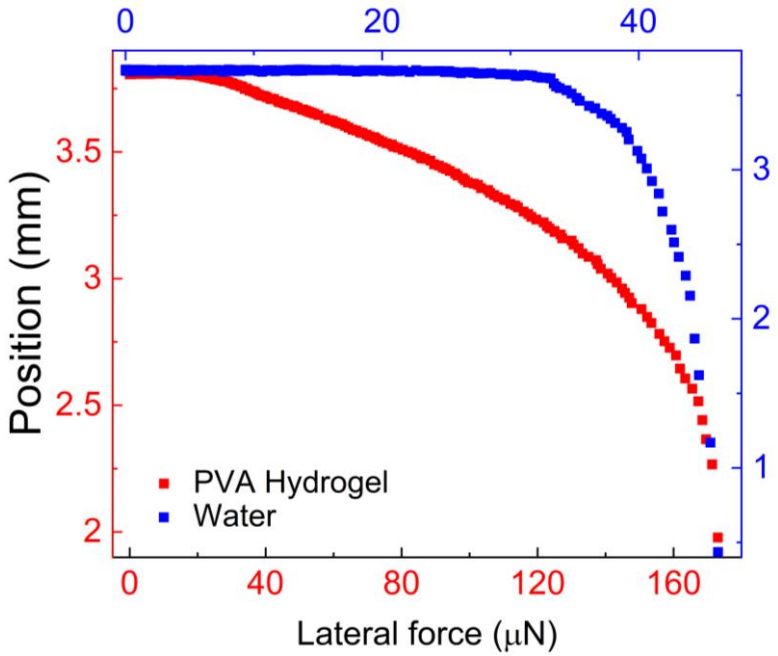

Figure 6. Determination of the lateral force needed to initiate motion of a PVA hydrogel drop on a hydrophobic, octadecyl-trimethoxy-silane coated silicon surface. The CAB rotates at a speed of 3rpm/sec.

We compared the force required to slide the hydrogel with the force required to slide a 3.0 µl water droplet. Figure 6 shows the change in drop position as the applied centrifugal force increases. The lateral force needed to initiate motion was determined when the advancing edge of the drop began to change its position even with a slight increase in centrifugal force.

This point is known as the onset of motion, and the centrifugal force acting on the drop at the onset of motion is referred to as the lateral force, $f_{\parallel}$. In our previous study [41], we determined the onset of motion based on a 0.5 mm translation of the drops from their initial position, resulting in a reported lateral force approximately 35 % lower than the value we reported in this paper. The lateral force, $f_{\parallel}$, required to slide the hydrogel drop was approximately 111 µN, whereas for water it was around 33.0 µN.

The higher lateral force observed for the hydrogel indicates stronger adhesion to the hydrophobic surface compared to water, highlighting the good mucoadhesivity of PVA. Additionally, Figure 6 provides valuable insights into the behavior of PVA hydrogel under lateral forces, which is relevant to applications such as drug delivery and wound dressing.

3. Synthetic Mucus Made by Polyvinyl Alcohol Crosslinked Using Borax

The PVA-Borax compound, a hydrogel composed of a three-dimensional network of hydrophilic polymers, has attracted significant attention from the biomedical and pharmaceutical industries due to its enhanced mechanical properties and biocompatibility. It finds applications in drug delivery, wound dressing, artificial cartilage materials, and other medical purpose [42].

 doi:10.20944/preprints202306.0172.v1

One of the most important features of this hydrogel is its ability to self -heal. Even after being broken apart, it can reform into a single continuous piece without additional external stimuli due to the reformation of hydrogen bonds which were broken down [43].

a) Rheological Properties of Polyvinyl Alcohol Hydrogels Crosslinked Using Boron

Lu et al. [44] investigated the rheological properties of PVA Borax hydrogels prepared using a 4.0 wt % PVA solution, in a frequency range of 0.01-10 Hz. As shown in Figure 7, they observed that all these samples exhibited viscous behavior at low frequencies and elastic behavior at high frequencies, indicating the presence of a reversible crosslinking network. The storage and loss moduli of the hydrogels crossed over at a frequency of 0.25 Hz.

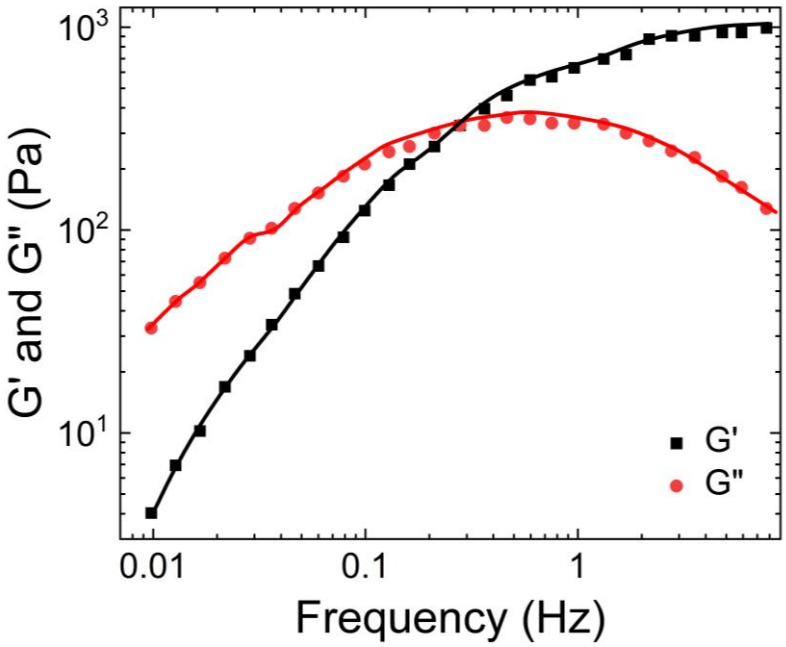

Figure 7. Storage modulus and loss modulus of PVA Borax hydrogel (4 wt % of PVA with 0.4 wt % of borax) with an increase in the shear frequency. (Plots reconstructed based on the Figure 6 from Lu et al. [44]).

Lin et al. [16] examined the dependence of the storage and loss moduli of a 6.0 wt% PVA Borax solution on shear rate. As shown in Figure 8, a crossover occurred between G′ and G″ at 2.40 Hz. Up to 2.40 Hz, the hydrogel exhibited a viscous nature (being G″ > G′), while beyond 2.40 Hz, it exhibited an elastic nature (being G″ < G′).

Preprints.org (www.preprints.org) | NOT PEER-REVIEWED | Posted: 2 June 2023 doi:10.20944/preprints202306.0172.v1

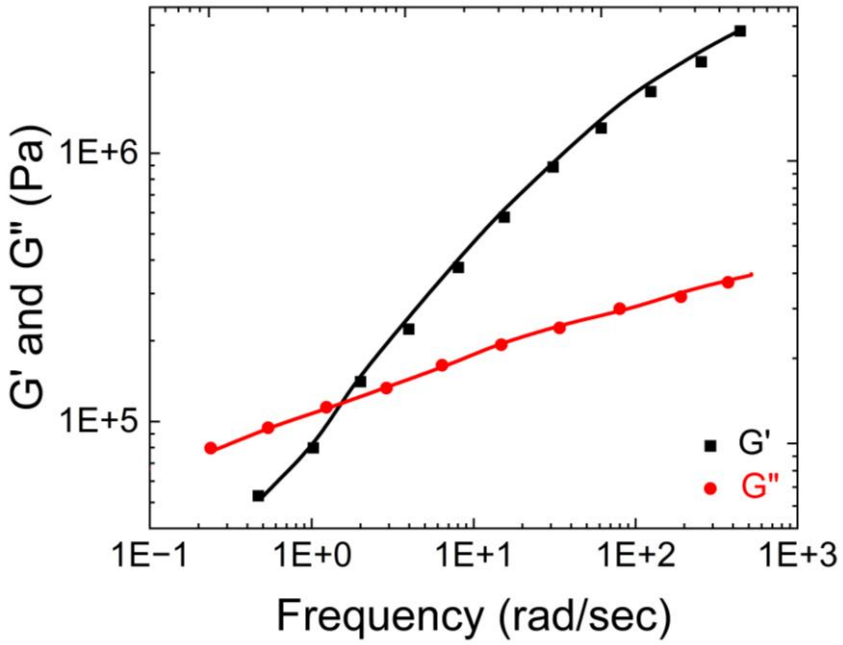

Figure 8. The storage and loss moduli of PVA Borax solution (60 g/L of PVA with 0.28 M of borax) at 60°C vs an increase in shear frequency. (Plots reproduced based on Figure 10 from Lin et al. [16]).

In our team's study, [41], we investigated the rheological properties of a PVA Borax hydrogel with a 1.0 wt % PVA solution. Figure 9 shows that the storage modulus (G′) was higher than the loss modulus (G″) of the hydrogel up to 8.90 Hz, beyond which a crossover between G′ and G″ occurred. These findings offer important insights into the rheological behavior of PVA Borax hydrogels and can certainly aid in the design of drug delivery and tissue engineering.

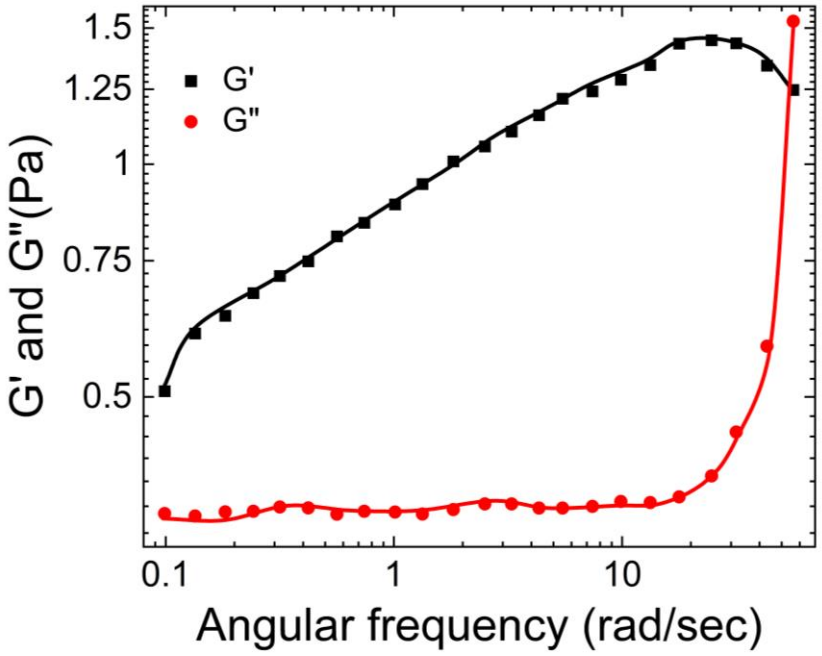

Figure 9. The storage (G′) and loss (G″) moduli of PVA Borax hydrogel (1 wt % of PVA with 1 wt % of borax mixed in a volumetric ratio of 10:1) vs an increase in shear frequency.

 doi:10.20944/preprints202306.0172.v1

b) Tribological Properties of Polyvinyl Alcohol Hydrogels Crosslinked Using Boron

Cui et al. [45] conducted a study on the tribological properties of PVA Borax hydrogel using a UMT-2 tribometer at room temperature. Their results demonstrated that pure PVA hydrogel exhibited the highest coefficient of friction, approximately 0.159. As the concentration of borax was increased in the PVA solution the coefficient of friction decreased, reaching its lowest value of 0.077 observed within the range of 0.3 to 0.4 wt %. However, beyond this range, the coefficient of friction started to increase with higher concentrations of borax.

Furthermore, Cui et al. also investigated the effects of normal load and sliding speed on the frictional properties of PVA Borax hydrogel coated on stainless steel balls. They observed that as the normal load increased from 2.0 to 8.0 N, the coefficient of friction increased from 0 to a range of 0.077 to 0.117. This phenomenon can be attributed to the increase in solid contact area between the hydrogel and the stainless-steel balls, resulting in complete extrusion of water from the hydrogel and subsequently increasing the friction coefficient.

Regarding sliding speed, the friction coefficient increased with higher sliding speeds. This can be attributed to the compression of the hydrogel during sliding, which forces water out of the gel network and leads to an increase in the friction coefficient.

In our study, Vinod et al. [41], the force required to initiate motion of a 3.0 µl PVA Borax hydrogel drop on a hydrophobic surface was investigated using CAB. The results are presented in Figure 10A–C.

Figure 10A provides a comparison of the lateral force needed to initiate motion for PVA Borax hydrogel and water. It can be observed that the force required to initiate motion is approximately 4 times higher for the hydrogel (166 µN) compared to water (39.0 µN).

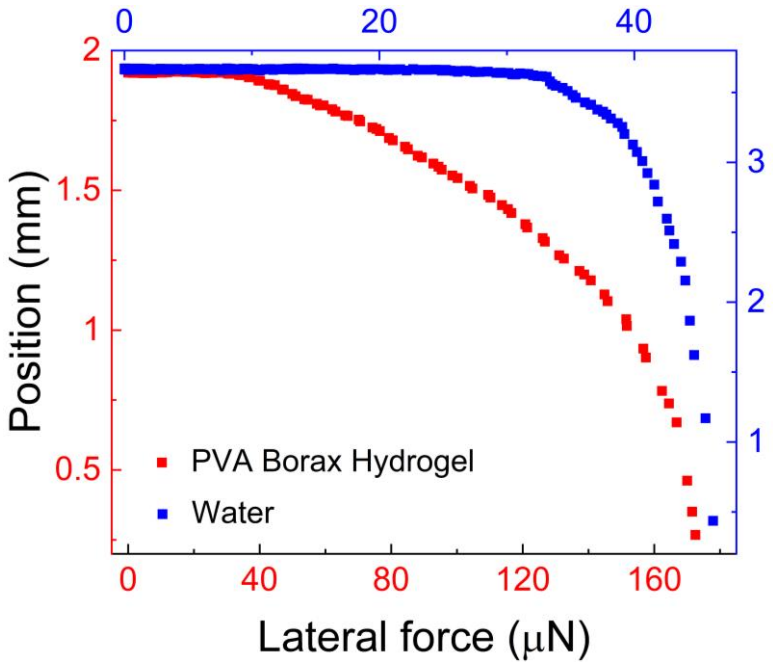

Figure 10. A. Determination of the lateral force needed to initiate a PVA Borax hydrogel drop motion on a hydrophobic surface made by coating octadecyl-trimethoxy-silane on silicon surface. The position at which the drop starts the motion is decided when the slope of the position curve starts declining with the slightest increase in the lateral force. CAB rotates at a speed of 3.0 rpm/sec.

The force versus t_{still} plots are shown in Figure 10B, revealing that the lateral retention force, f_l, necessary to initiate sliding of the hydrogel drops consistently exceeds that of pure water. This observation aligns with the adhesive properties of mucus, which has a tendency to capture hydrophobic particles. In this context, the higher force required to slide the hydrogel on the

Preprints.org (www.preprints.org) | NOT PEER-REVIEWED | Posted: 2 June 2023 doi:10.20944/preprints202306.0172.v1

hydrophobic particle (represented by octadecyl-trimethoxy-silane on silicon surface) further supports its sticky nature. Notably, the hydrogel exhibits such strong adhesion that it does not fully detach from the solid surface on which it slides, specifically the silanized silicon surface.

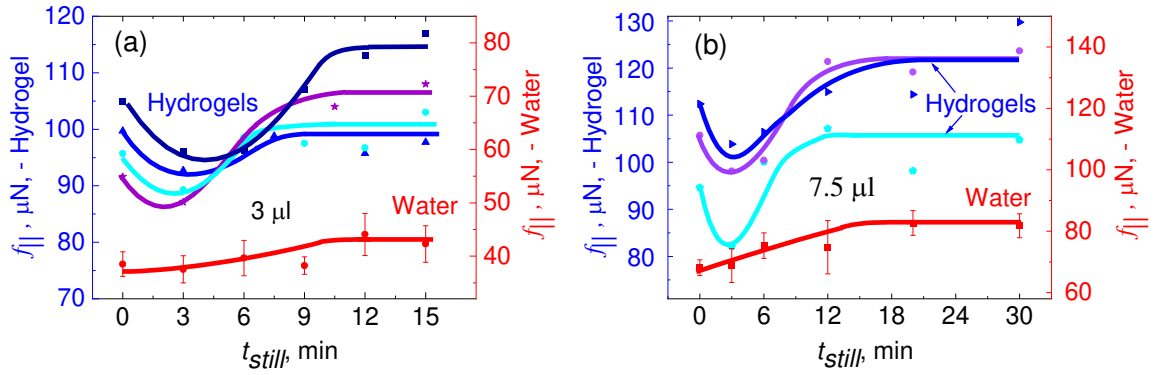

Figure 10. B. Variation of lateral force, $f_{||}$, with the increase in still time, t_{still}, for hydrogels (shades of blue) and for water (red color) on C18 silanized silicon surface. The dots show experimental data from different runs of **(a)** 3.0 µl and **(b)** 7.5 µl. The water data points represent average of three different runs of the corresponding volumes. The gel data (blue lines) represent individual runs without averaging. Beyond the scatter, the different bluish curves show reproducibility of the minimum around 3 minutes. The solid lines are guides to the eye. (The plot is printed after getting permission from Vinod et al. [41]).

Given the PVA Borax hydrogel's inherently adhesive properties, it is anticipated to exhibit a greater work of adhesion compared to water. To verify this assumption, Figure 10C illustrates the work required to detach drops of PVA Borax hydrogel and water from the underlying solid surface, along with the corresponding calculation of the work of adhesion. Notably, the data indicates that a higher force and work of adhesion are necessary to separate the hydrogel from the silanized silicon surface in comparison to water.

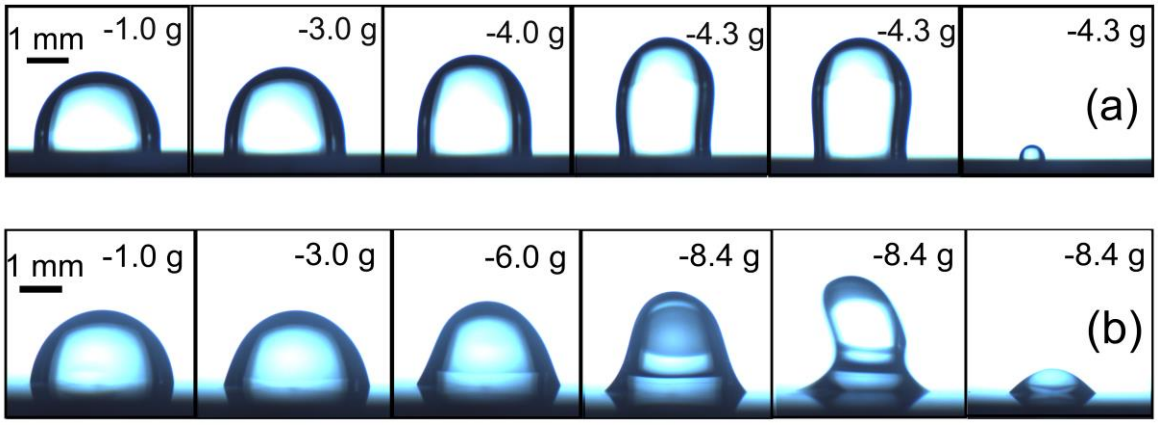

Preprints.org (www.preprints.org) | NOT PEER-REVIEWED | Posted: 2 June 2023 doi:10.20944/preprints202306.0172.v1

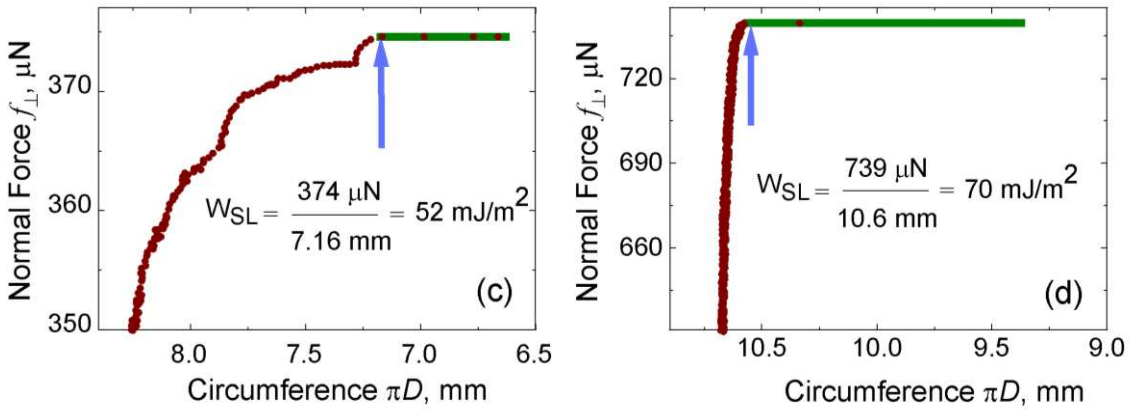

Figure 10. C. The triple line circumference of 8.0 μl drops on C18 silanized silicon surface versus the effective gravitation force pulling the drops. **(a)** Water drop **(b)** hydrogel (0 t_{still}). The blue arrows point on the data taken for the calculation of the work of adhesion, i.e., when the drops' diameter reduces spontaneously with no increase in normal force. The experiments were conducted using CAB runs at 1 rpm/sec. Image strips of drops with corresponding effective gravitation force pulling on them (c) water and (d) PVA hydrogel (0 t_{still}). (The plot is printed after getting permission from Vinod et al. [41]).

The work of adhesion, calculated for water is 52 mJ/m² (as shown in Figure 10(Cc)), and the work of adhesion calculated for PVA Borax hydrogel is 70 mJ/m² (as shown in Figure 10(Cd)).

The data presented in Figures 6 and 10, can be used to optimize the design of hydrogel-based devices by determining the minimum force required to initiate motion of the hydrogel.

4. Synthetic Mucus Made by Using Guar Gum

Guar gum, derived from the natural seed of Cyamopsis tetragonolobus [46] stands out from other plant gums due to its unique characteristic of lacking uronic acid [47,48]. Despite its relatively low concentration, guar gum exhibits high shear viscosities, and its hydrogel solutions display shear thinning behavior, where viscosity decreases with applied shear stress [49]. Guar gum finds practical applications in the fields such as food industry, oil recovery and in skin care industries [50]. It serves as a mucus-like agent for colon delivery and as a matrix for oral solid dosage forms [51,52].

Due to its branched structure, guar gum readily hydrates but does not allow extensive hydrogen bonding between the guar macromolecules [53]. Although it doesn't readily form a gel, guar gum is widely used as thickener.

(i) Guar Gum with Scleroglucan

Scleroglucan is a water-soluble polysaccharide that finds various commercial applications in fields such as secondary oil recovery, ceramic glazes, food, paints, cosmetics etc. [51].

a) Rheological Properties of Guar Gum and Scleroglucan Mucus Simulant

Zahm et al. studied the viscoelastic properties of a hydrogel composed of guar gum and scleroglucan using a steady shear viscoelastometer [54] at a shear rate of 0.4 s^{-1} and 1.6 s^{-1}. They observed a significant decrease in viscosity as the shear rate increased. The simulated mucus showed a notable reduction in viscosity during shearing, making it easier for the mucus to be transported from the airway. The decrease in viscosity is attributed to changes in the physical crosslinking of the macromolecules that constitute the simulated mucus. This molecular bond breakage and associated viscosity reduction have also been reported by Quedama and Droz [55].

Lafforgue et al. [56] synthesized the same hydrogel as Zahm et al., and conducted rheological and tribological studies on it. They performed rheological experiments using AR 550 (TA

 doi:10.20944/preprints202306.0172.v1

instruments), with a 50 mm/ 2° steel cone. The viscoelastic properties of the mucus simulant were determined by studying the storage (G′) and loss (G″) moduli of the mucus as a function of the oscillating stress amplitude. Their results, as shown in Figure 11, indicate that the G′ values of the mucus simulant are consistently higher than its G″ values until the yield point. Beyond the yield point, the behavior of G′ and G″ changes as the gel network starts to breakdown. At a certain point, G″ surpasses G′, indicating that the material becomes more viscous than elastic. This transition occurs due to the structural breakdown of the hydrogel.

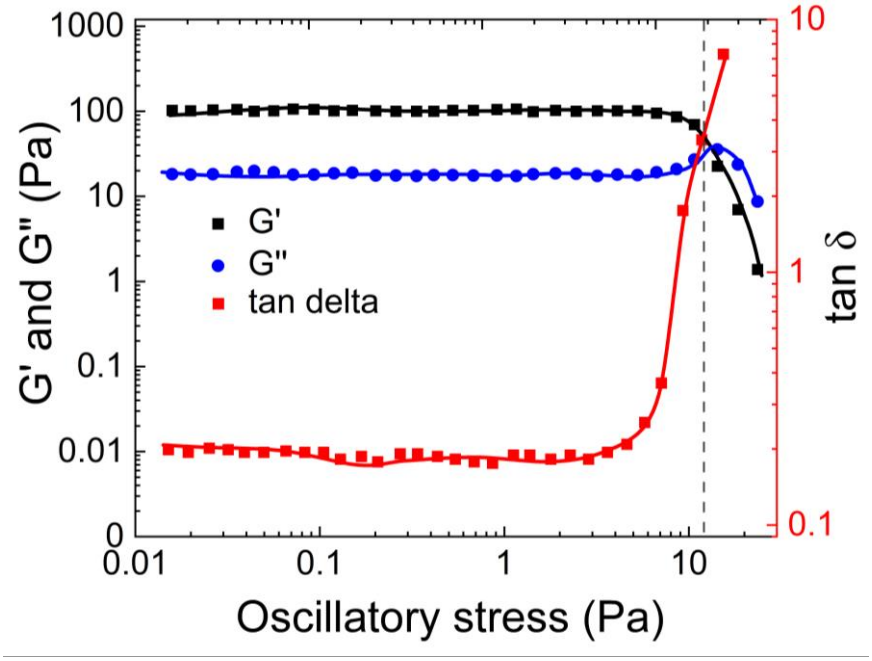

Figure 11. The storage (G′) modulus, loss modulus (G″), and the loss factor for 1.5 wt% concentration of scleroglucan obtained at 20°C as a function of the stress amplitude at a constant frequency of 1 rad/sec. (The plot is reconstructed based on the Figure 4 from Lafforgue et al. [56]).

Lafforgue et al. made a same observation to Zahm et al. and Mezger et al. [57] regarding an overshoot in the viscous modulus after the yield point. This overshoot occurs due to the energy dissipation resulting from the breakage of the network that holds the hydrogel together. This variation in G′ and G″ with oscillatory stress, and the overshoot of G″ at the yield point is consistent with the findings of Lai et al. [58].

b) Tribological Properties of Mucus Simulated Using Guar Gum and Scleroglucan Mucus Simulant)

Lafforgue et al. conducted measurements of the surface tension of the mucus simulant, consisting of guar gum and scleroglucan, using a du Nouy ring [56]. Their findings indicated that the surface tension of the mucus simulated varied from 71.6 to 89.9 mN/m, corresponding to scleroglucan concentrations ranging from 0.5 % to 2.0 % respectively.

(ii) Guar Gum with Borax

The hydrogel synthesized using guar gum and borax has been previously studied by several groups [59,60]. They have investigated how the rheological properties of the hydrogel depends on various factors, such as polymer compositions, temperature, and environmental pH conditions. Borax plays a crucial role in promoting rapid gelation of guar gum by forming crosslinks with a lifetime on the order of seconds, which contributes to the self-healing properties of this network. The reversible chemical bridges formed between the chains of guar gum through crosslinking with borax are responsible for its unique characteristics [50].

 doi:10.20944/preprints202306.0172.v1

a) Rheological Properties of Guar Gum with Borax

Coviello et al. [50] conducted rheological characterization of the guar gum borax hydrogel using a controlled stress rheometer, the Haake Rheo-stress RS 300 model, at 25°C and 37°C. As shown in Figure 12, at 25°C, the storage modulus (G′) was consistently higher than the loss modulus (G″), indicating the elastic nature of the hydrogel. However, at 37°C, both moduli increased, and the the loss modulus surpassed the storage modulus at a crossover point of $\omega = 0.2$ rad/sec.

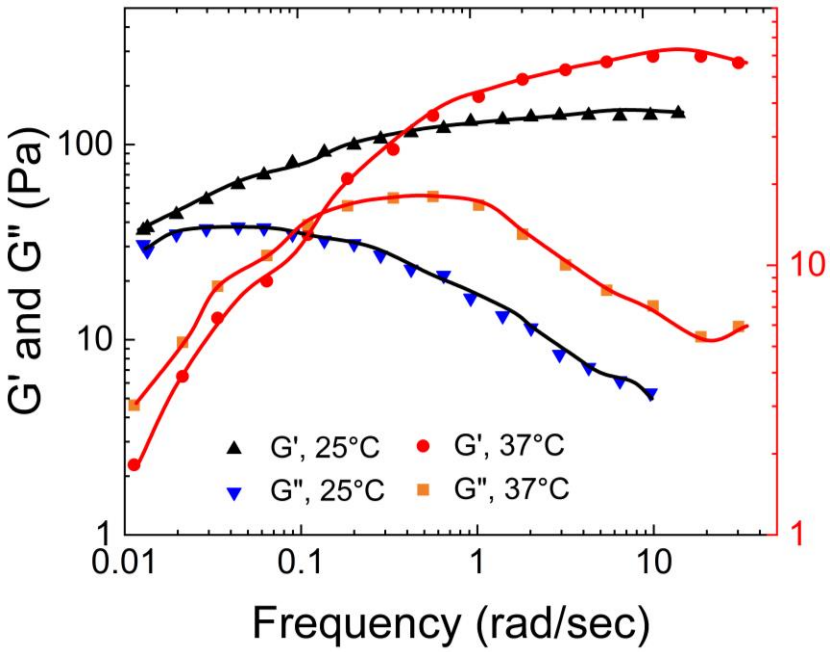

Figure 12. The storage modulus (G′) and loss modulus (G″) of guar gum with borax vs shear frequency at 25°C and 37 °C. The black shades represent 25°C, and the red shades represent 37°C. (Plots reproduced based on Figures 4 and 5 of Coviello et al. [50]).

Pan et al. [61] also characterized the rheological properties of the guar gum borax hydrogel. As shown in Figure 13, they observed that the storage modulus of the hydrogel was bigger than the loss modulus. Moreover, G′ remained relatively constant with an increase in the frequency, while G″ exhibited a slight decrease.

Preprints.org (www.preprints.org) | NOT PEER-REVIEWED | Posted: 2 June 2023 doi:10.20944/preprints202306.0172.v1

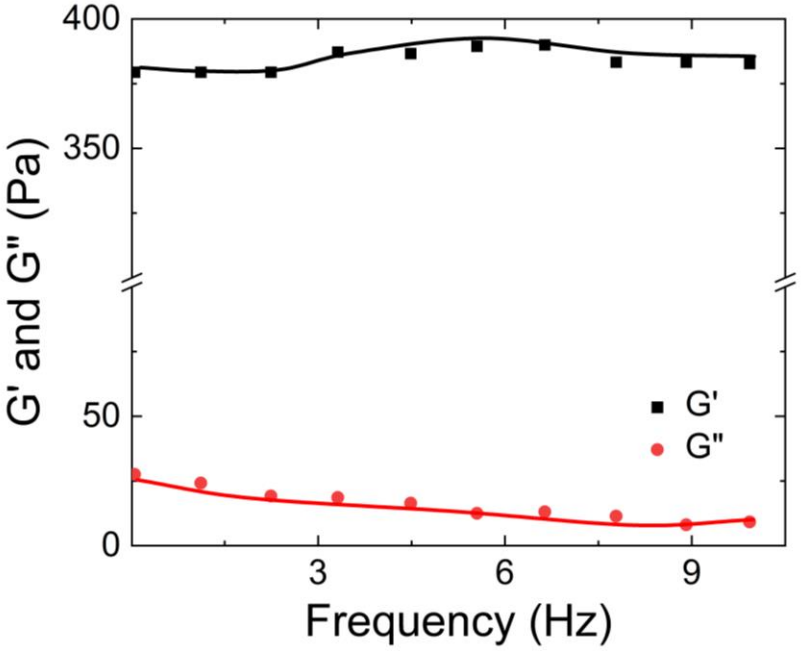

Figure 13. Storage modulus G′ and loss modulus G″ of guar gum with borax hydrogel versus shear frequency. (Plot reconstructed using Figure 6 from Pan et al. [61]).

Sun et al. [62] also investigated the rheological properties of the guar gum-borax hydrogel. They studied the dependence of its apparent viscosity on the shear rate, as well as the dependency of its storage and loss moduli on the shear. As shown in Figure 14, they found that the viscosity of the guar gum solution was approximately 0.1 Pa.s and remained independent of the shear applied. In contrast, the apparent viscosity of the guar gum with borax increased with increasing shear rate. Additionally, as shown in Figure 15, the storage modulus (G′) of the hydrogel was higher than the loss modulus (G″). The crossover frequency occurred at 36 rad/sec.

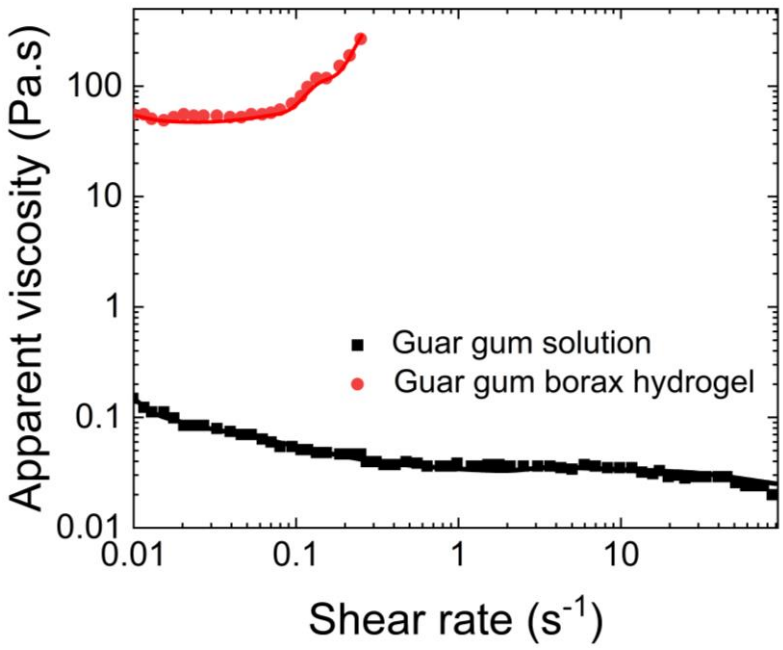

Figure 14. Comparison between the apparent viscosities and shear rate of guar gum solution to guar gum borax hydrogel. (Plots reproduced based on Figure 3 of Sun et al. [62]).

 doi:10.20944/preprints202306.0172.v1

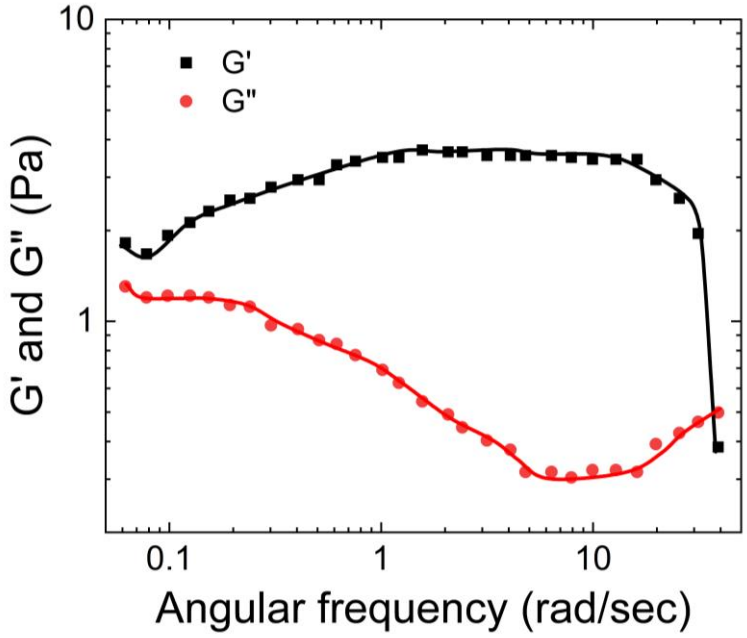

Figure 15. Storage and loss moduli vs increase in the shear frequency of guar gum hydrogel crosslinked using borax. (Plot reconstructed based Figure 7 of Sun et al. [62]).

a) Tribological Properties of Mucus Simulated Using Guar Gum and Borax

Pan et al. [61] conducted a study on the adhesive properties of a borax crosslinked guar gum hydrogel. Adhesion tests were performed using a digital tensile machine, where the hydrogel was applied onto a metal sheet coated with a surface mimicking human skin, and then pulled until detachment occurred. The results indicated that a work of adhesion of 2.5 KPa was required to detach the hydrogel from the 'human skin mimicking surface'. This observation suggests that the hydroxyl groups in the crosslinked guar gum hydrogel have the ability to form hydrogen bonds with the surface, mimicking the interaction with human skin.

5. Synthetic Mucus Based on Polyglycerol

Linear poly glycerol is used as a base for developing synthetic hydrogels due to the presence of pendant hydroxyl groups in them. Bej et al. [63] reported effectiveness of sulfated linear polyglycerol as an excellent inhibitor against respiratory diseases such as HSV-1 and COVID 19. Furthermore, hydrogels based on linear polyglycerol (LPG) have been used as bioinert 3D matrices for pluripotent stem cells due to their ability to form a porous network similar to native mucus. In this context, we will discuss the rheological and tribological properties of these synthetic mucus simulants.

a) Rheological Properties of Linear Poly Glycerol Based Synthetic Hydrogel

Sharma et al. [64] investigated the viscoelastic properties of three different Mucus Inspired Hydrogels (MIHs), named MIH-1, MIH-2, and MIH-3 that contain reversible, redox-responsive bonds similar to those found in native mucus.

MIH-1, MIH-2, and MIH-3 differ in the linear polyglycol backbone and the crosslinker ratio used in their synthesis. MIH-1a, MIH-1b, MIH-1c, and MIH-1d represent variations in the crosslinker (Mucin) to linear component (Polyglycerol (PEG-1)) ratio (1:3, 1:7, 1:10, and 1:14, respectively). MIH-2 (PEG-2: Mucin =3:1) and MIH-3 (PEG-3: Mucin =3:1) exhibit different linear polyglycol backbones.

PEG-1 is obtained after acidic and basic hydrolysis of ethoxy ethyl and thiourea group, PEG-2 is synthesized following an approach modified from the original report from Mahadevagowda and Stuparu [65], and PEG-3 is prepared using homo bifunctional dihydroxy PEGs, a detailed

 doi:10.20944/preprints202306.0172.v1

description of its preparation is given in the reference [64]. The rheological properties of these MIHs were characterized by storage (G′) and loss (G″) moduli obtained from oscillatory shear experiments conducted at 25°C and 37°C.

As shown in Figure 16, for MIH-1 (data presented in Figure 16 is an average of MIH-1a, MIH-1b, MIH-1c, and MIH-1d), both G′ and G″ increased by more than a factor of 10 as the temperature increased, with a more pronounced effect on G′. This indicates an increase in the elastic property of the gel with temperature.

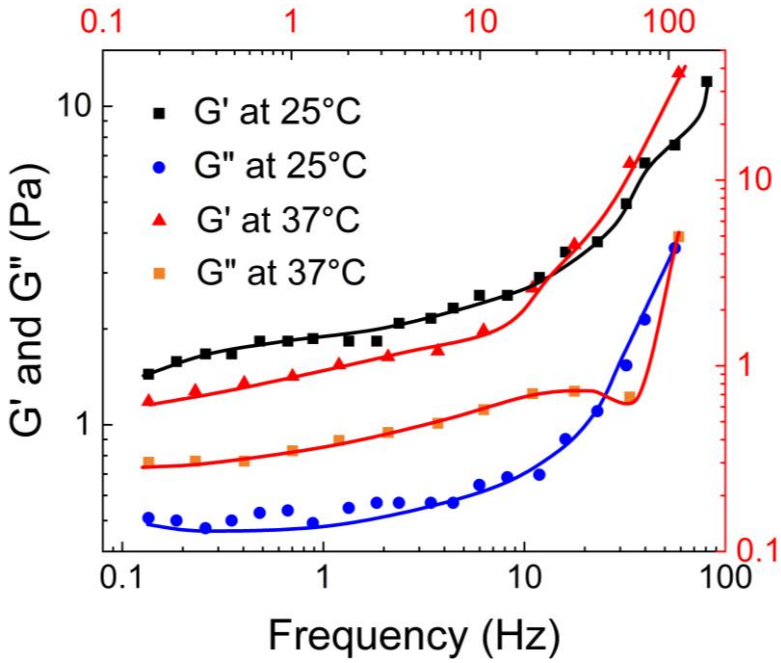

Figure 16. The storage modulus and loss modulus of MIH-1 hydrogels vs shear applied at 25°C and 37°C. The black shades represent experiments at 25°C, and the red shades represent experiments at 37°C. (Plots were reconstructed using Figure 4 of Sharma et al. [64]).

For MIH-2, as shown in Figure 17, both G′ and G″ exhibited a linear increase with increasing shear, indicating a gel dominated by its viscous characteristics, resembling a soft, gel-like viscoelastic fluid. The moduli also increased by a factor of 10 with increasing temperature.

Preprints.org (www.preprints.org) | NOT PEER-REVIEWED | Posted: 2 June 2023 doi:10.20944/preprints202306.0172.v1

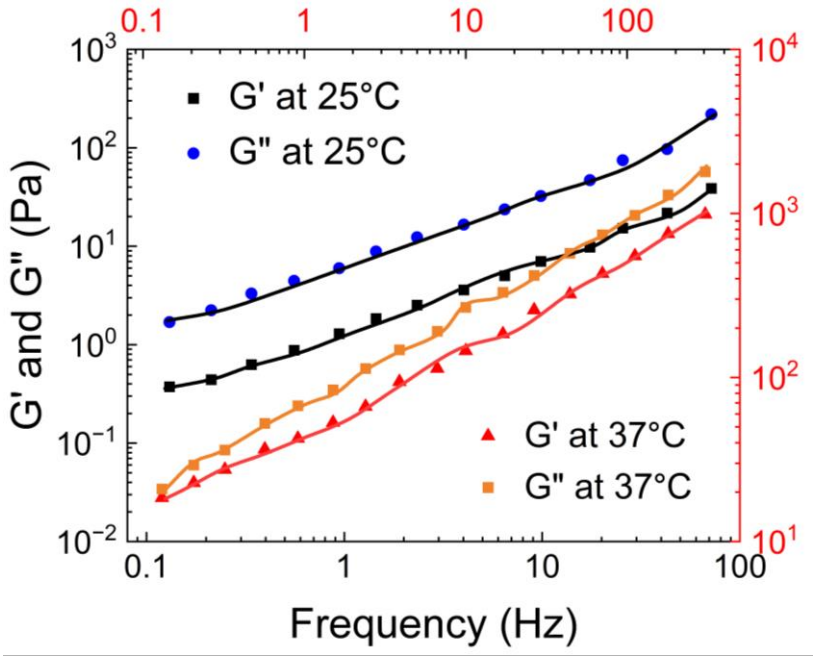

Figure 17. Storage (G′) and loss (G″) moduli as a function of the shear induced at 25°C and 37°C. The black shades represent data from experiment conducted at 25°C, and the red shades represent data from experiment conducted at 37°C. (The plot is reconstructed based on the Figure 2 of Sharma et al. [64]).

In Figure 18, it is evident that the storage and loss moduli of MIH-3 increase almost linearly with the shear rate. For MIH-3 synthesized at 25°C and 37°C, the loss modulus surpasses the storage modulus. Moreover, as the temperature rises from 25°C to 37°C, both moduli show a significant increase.

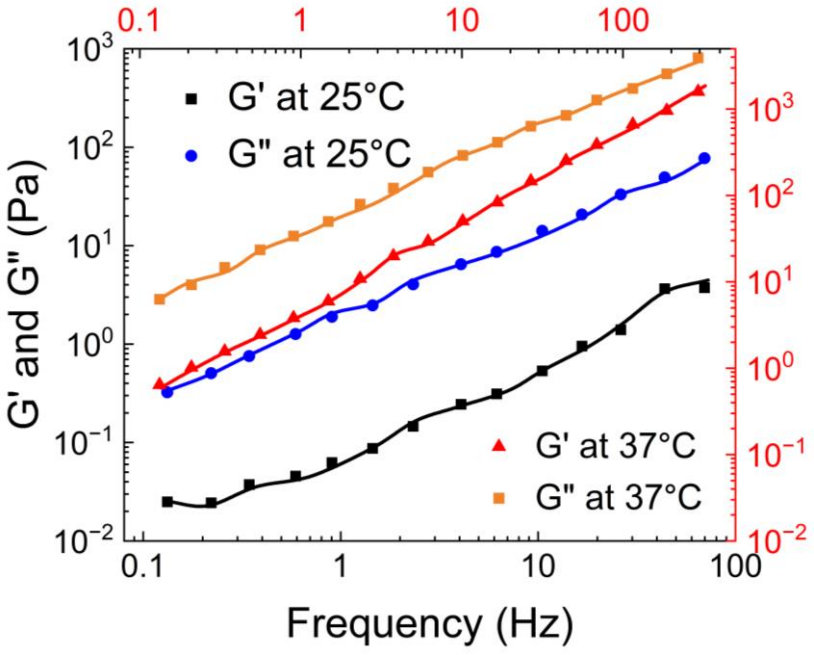

Figure 18. The relationship between the storage (G′) and loss (G″) moduli of MIH-3 at different shear frequencies, measured at 25°C and 37°C. The black shades represent data from experiments

 doi:10.20944/preprints202306.0172.v1

conducted at 25°C, while the red shades represent data from experiments conducted at 37°C. (The plot is reconstructed based on the Figure 2 of Sharma et al. [64]).

In a similar rheological study, Lospichl et al. [66] examined the viscoelastic properties of polyglycerol sulfate hydrogels. As shown in Figure 19, they observed pronounced gel-like behavior in all tested gel samples, with G′ significantly exceeding G″, aligning with Sharma et al.'s findings regarding MIH-1 hydrogels.

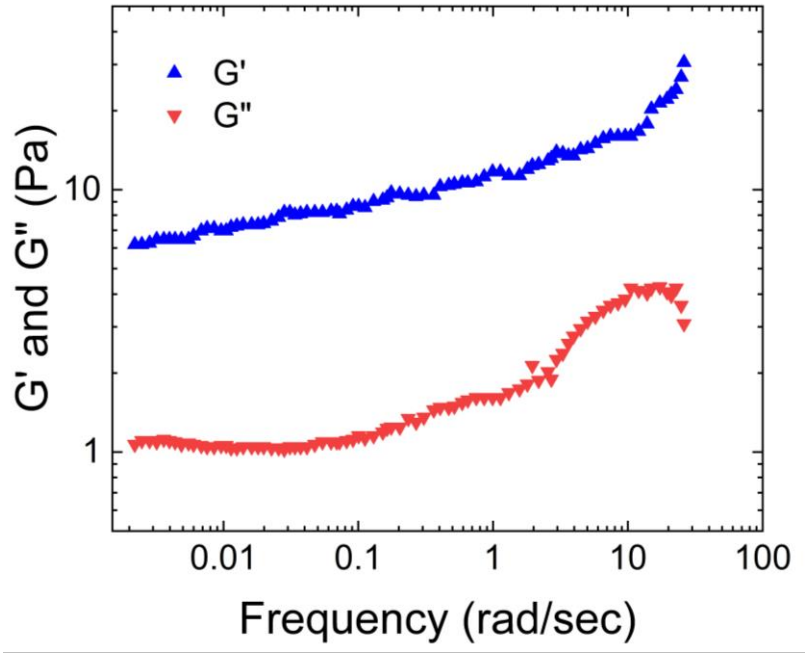

Figure 19. The storage modulus (G′) and loss modulus (G″) of 3.6 wt % dPGS hydrogels as a function of shear applied. (The plots were reconstructed using Figure 4 of Lospichl et al. [66]).

Furthermore, Ekinci et al. [67] investigated the rheological properties of a polyglycerol-based polymer network using a rheometer equipped with an external UV-light source. As demonstrated in Figure 20, they observed that G″ surpassed G′, indicating a viscous fluid behavior. This finding of Ekinci et al. is consistent with Sharma et al.'s observations regarding MIH-2 and MIH 3 hydrogels.

 doi:10.20944/preprints202306.0172.v1

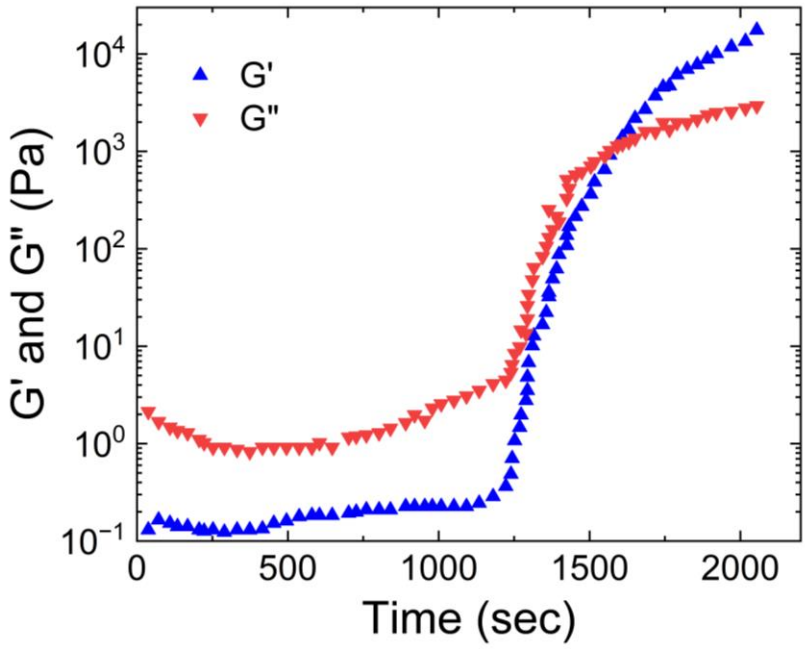

Figure 20. Evolution of the storage (G′) and loss (G″) moduli during the polymerization and hardening of 0.1 wt% of Glycerol glycidyl ether. (The plot was reconstructed based on Figure 4 of Ekinci et al. [67]).

The key distinction among the systems studied by Sharma et al., and Lospichl et al., and Ekinci et al. is that Sharma et al. and Lospichl et al. employed linear polyglycerol-based hydrogels, while Ekinci et al. used branched polyglycerol-based hydrogels.

b) Tribological Properties of Linear Glycerol-Based Polymers

Le at al [68] conducted a study on the tribological properties of glycerol solutions with added aluminum nanoparticles. They prepared an aqueous glycerol solution by mixing deionized water with glycerol to create a 10-50 wt% solution. Tribological experiments were performed using a thrust collar tribotester to measure the coefficient of friction and wear rate. The researchers discovered that an optimal concentration of aluminum nanoparticles in the glycerol solution resulted in the reduction in the coefficient of friction. The reduction can be attributed to the deposition of an aluminum film on the wear surface and the bearing ball effect of nanoparticles.

Orafai et al. [69] investigated the surface energy of poly (glycerol adipate) polymers by measuring contact angles with different test liquids [70,71] and plugging them into the Fowkes equation [72]. The researchers found that the surface energy of the polymer didn't have a pattern-based change with increasing adipate concentration in the polymer. Specifically, at an adipate concentration of 0 %, the surface energy was 62.41 mJ/m. At an adipate concentration of 20 %, the surface energy was 60.70 mJ/m. For an adipate concentration of 40 %, the surface energy was 31.38 mJ/m. Finally, at an adipate concentration of 100 %, the surface energy was 57.26 mJ/m. These data indicate that the addition of 40 % adipate to the poly glycerol polymer resulted in the lowest total surface free energy.

6. Synthetic Mucus Made by Polyacrylic Acid Hydrogels/Carbopols

Poly acrylic acid (PAA) hydrogels attracted considerable attention in the recent years due to their unique properties (ability to form gels, pH sensitivity) [73], and potential applications in various fields such as drug delivery, tissue engineering, and biosensors [74]. PAA hydrogels are characterized for their ability to absorb large amounts of water while holding their structural

 doi:10.20944/preprints202306.0172.v1

integrity. Due to their biocompatibility, PAA hydrogels is a good candidate for many biomedical applications [75].

Most recently, a polymeric combination called Carbopols has been developed which is made by crosslinking polyacrylic acid polymers with crosslinkers [76]. Rheological analysis of Carbopol is important, as its mucoadhesive ability is significantly depends on it [77–79]. Early studies on Carbopol showed that their distinct rheological properties depend on the entanglements of the high molecular weight polyacrylate molecules.

a) Rheological Properties of Poly Acrylic Acid Hydrogels

Kim et al. [80] conducted a study on the rheology of Carbopol using a Parr Physica UDS 200 mechanical rheometer at room temperature. They measured the storage (G′) and loss (G″) moduli in the linear viscoelastic regime during the frequency sweep tests. Figure 21 reveals that for PAA hydrogels, the storage modulus G′ consistently exceeded loss modulus G″. This low storage modulus was attributed to the flexible network structure and high-water content of the Carbopol macromolecule. At low frequencies, PAA hydrogels exhibited predominantly viscous behavior at low frequencies, while at high frequencies, the elastic nature dominated, resulting in a higher storage modulus. The loss modulus indicated a more dominant viscous behavior during deformation.

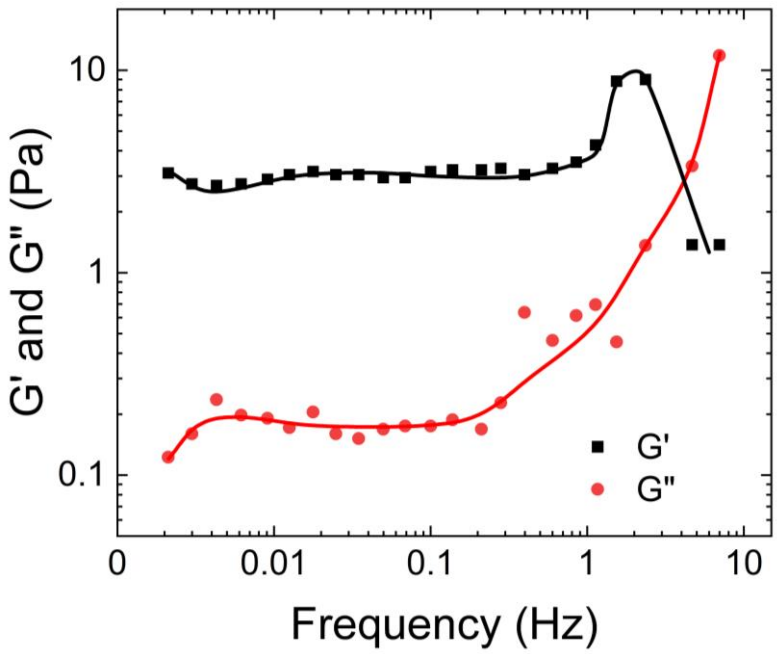

Figure 21. The storage modulus (G′) and loss modulus (G″) vs shear applied for a sample containing 4.0 wt% of Carbopol. (The plots are reconstructed using Figure 4 from Kim et al. [80]).

Bonacucina et al. [81], investigated the rheological properties of Carbopol as a function of shear and temperature using a stress control rheometer equipped with a cone-plate geometry. They compared the physical properties of two Carbopol samples, one synthesized at room temperature and the other at 70°C. Figure 22 illustrates that the sample synthesized at 70°C displayed gel-like behavior, with the storage modulus (G′) consistently surpassing the loss modulus (G″) across the entire frequency range tested, and both moduli remained independent of the change in frequency.

 doi:10.20944/preprints202306.0172.v1

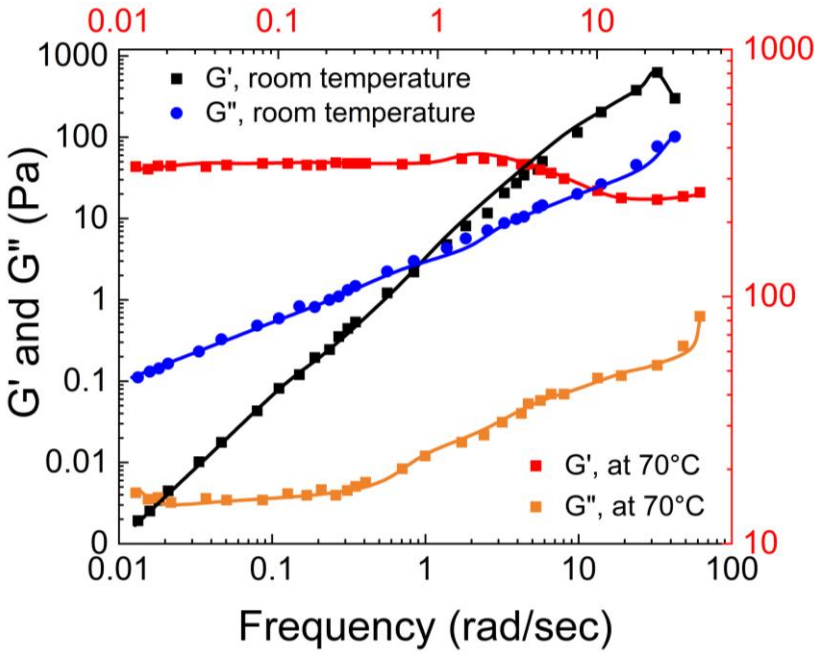

Figure 22. Frequency sweep of Carbopol gels in water prepared at room temperature and at 70°C. The black shades represent hydrogel samples synthesized at room temperature, and the red shades represent hydrogel samples synthesized at 70°C. (The plot is reconstructed based on Figures 3 and 7 from Bonacucina et al. [81]).

This frequency sweep test indicates that heating transforms Carbopol from a low viscosity semi-dilute solution to a gel-like structure, likely due to increased polymer-solvent interactions. Conversely, the frequency sweep test conducted on samples prepared at room temperature revealed that the loss modulus consistently exceeded the storage modulus, which is typical for a semi-dilute polymer solution. Therefore, Carbopol synthesized at room temperature by Bonacucina et al. cannot be used as a drug delivery agent since it does not exhibit gel-like behavior.

Baek et al. [82] conducted rheological measurements on different concentrations of Carbopol using a stress-controlled rheometer (AR 2000, TA Instruments). Figure 23 demonstrates that the storage modulus (G′) consistently exceeded the loss modulus (G″), indicating the elastic behavior of Carbopol.

 doi:10.20944/preprints202306.0172.v1

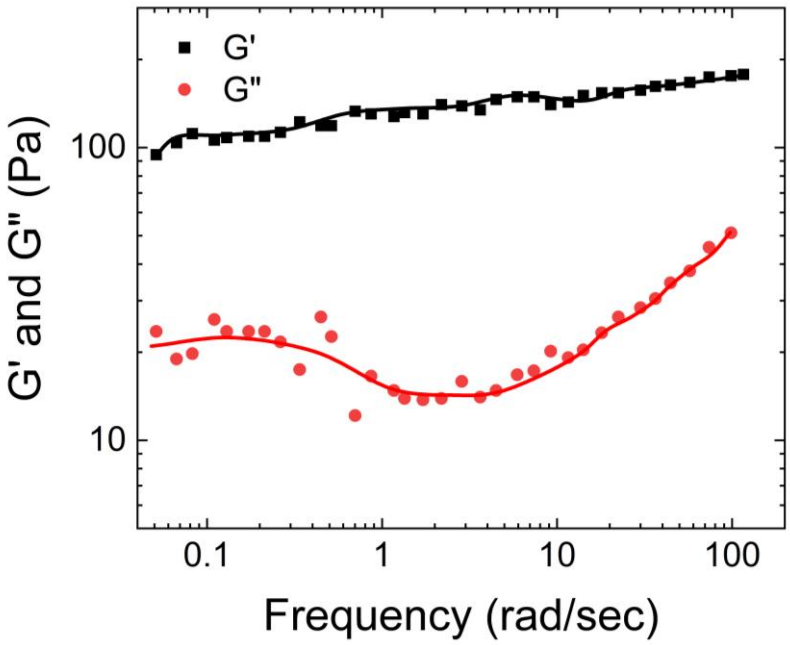

Figure 23. The storage modulus (G′) and loss modulus (G″) as function of shear applied for pure Carbopol of concentration 0.25 wt%.

Schenck et al. [83] investigated the rheological properties of Carbopol hydrogels with concentrations ranging from 0.025% to 0.05%. According to Figure 24, they observed that both the storage and loss moduli were dependent on the frequency of the applied shear. For all gel concentrations, the moduli increased as the shear frequency increased from 0.5 to 105 rad/sec. A significant increase in G′ and G″ was noticed at 10 rad/sec, which continued up to frequencies of 105 rad/sec. This sharp increase in the rheological moduli values at 10 rad/sec was attributed to the breakdown of the gel structure, indicating the gel's ability to relax at high deformation frequencies. This behavior is commonly observed in semiflexible polymer networks [84] and mucus simulants [54]. Furthermore, the viscoelastic moduli of the Carbopol hydrogel increased with higher Carbopol percentages in the hydrogel. The values of G′ and G″ for 0.03%, 0.04%, and 0.05% gels fell within the reported ranges for native, healthy and tracheobronchial mucus samples [85].

 doi:10.20944/preprints202306.0172.v1

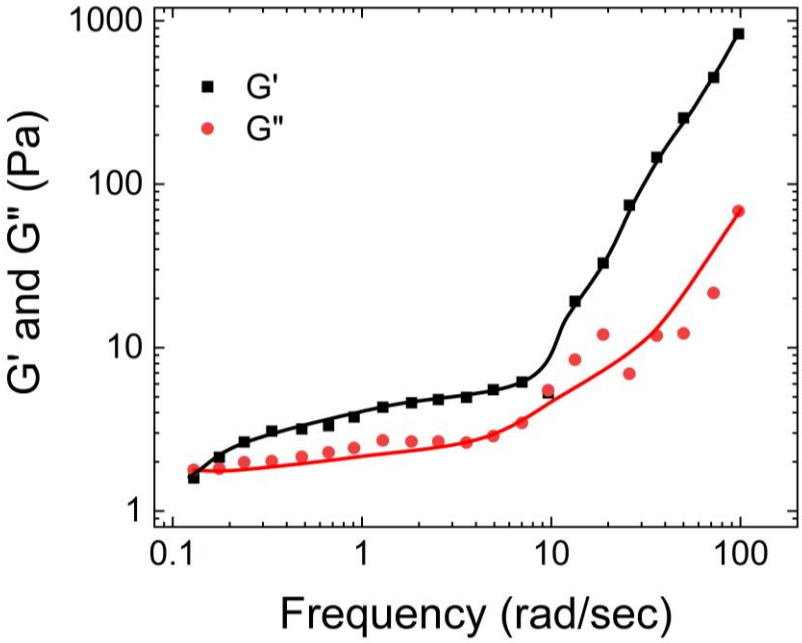

Figure 24. Frequency dependence of the storage modulus (G′) and the loss modulus (G″) for neutralized Carbopol of 0.04 wt%. (The plot was reconstructed based on Figure 1 of Schenck et al. [83]).

Vicente et al. [86] also conducted rheological studies on Carbopol at 35°C using both controlled-strain (Rheometrics ARES-LS rheometer) and controlled-stress (Haake RS1) rheometer. They used a concentration of 0.1% of Carbopol in the hydrogel. As shown in Figure 25, G′ was consistently higher than G″. It is worth noting that the storage modulus value remained nearly constant throughout the frequency range, with a slight increase in the loss modulus values around 10 rad/sec. This observation aligns with the findings of Schenck et al., who also reported a sharp increase in the loss modulus above 10 rad/sec.

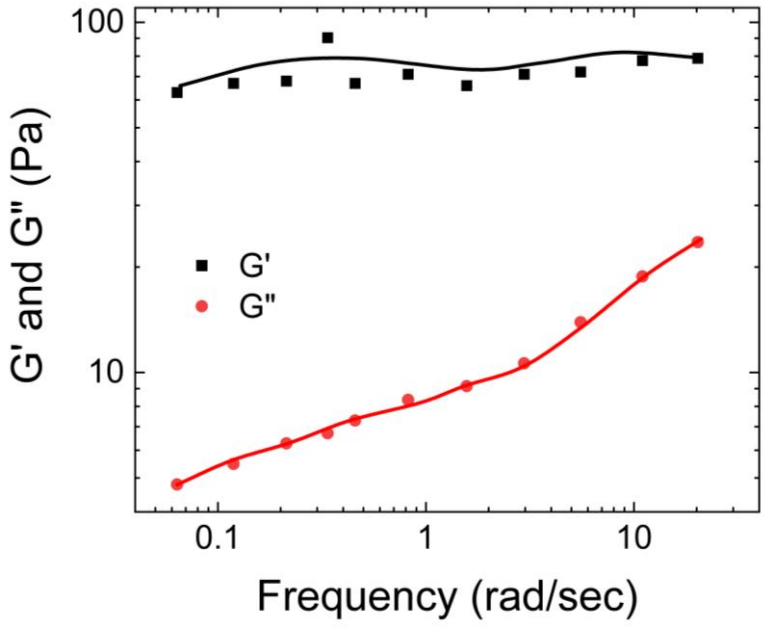

Figure 25. Rheology of neutralized Carbopol (0.2 wt%) vs dynamic oscillatory shear in the viscoelastic linear regime. (The plot was reconstructed based on Figure 3 of Vicente et al. [86]).

 doi:10.20944/preprints202306.0172.v1

a) Tribological Properties of Poly Acrylic Acid Hydrogels

The surface tension of Carbopol hydrogel was expected to be close to that of water (~72 mN/m) due to its high-water content. Furthermore, Carbopol is not surface active, which further supports this expectation. Schenck et al. conducted experiments to measure the surface tensions of the hydrogel at different concentrations of Carbopol, obtaining values such as 2.33± 0.12, 71.63± 0.23, and 71.77± 0.37 mN/m for concentrations of 0.025%, 0.04% and 0.05%.

Vicente et al. [86] investigated the influence of rheology and polymer conformation on the tribological properties of Carbopol hydrogels by comparing the measured friction against the Newtonian master curve. They observed that at low entrainment speed, unneutralized Carbopol hydrogels exhibited similar friction coefficients to those of water, while at high entrainment speeds, the friction coefficients for all Carbopol hydrogels were lower than that of water.

Chau et al. [87] studied the pH dependence of the friction coefficient of polyacrylic acid hydrogel. They conducted tribological experiments using a linear reciprocating tribometer and found that the friction coefficients of the hydrogels could be altered by varying the hydrogel's pH and acrylic acid concentration. The friction coefficients ranged from 0.17±0.01 (at pH=0.35 and 0 wt% acrylic acid) to 0.005±0.001 (at pH=7 and 12 wt% acrylic acid) and decreased with increasing pH across all acrylic acid concentrations, except at 12 wt%. These results were consistent with those of Ma et al. [91], who observed friction coefficient ranging from 0.3-0.4 at a pH of 2 for their polyacrylic acid hydrogel, with low coefficients of friction observed at a pH of 12, as in Chau et al.'s study.

Discussion and Summary

In drug delivery systems, hydrogels are used as carriers to encapsulate and release therapeutic agents [88,89]. The rheological moduli of the hydrogel influence the drug release kinetics, and the release behavior of the loaded drug [90]. A hydrogel with a higher storage modulus (G') is generally associated with a more rigid structure, which leads to a slower release rate of the drug [91,92]. This happens because the drug molecules face higher resistance to diffuse through the hydrogel's network. Whereas a hydrogel with a higher loss modulus allows a faster drug diffusion and release due to its high viscous behavior [93].

Along with this, the rheological moduli of hydrogels also affect their interactions with biological tissues [94]. The mechanical properties of natural tissues are better imitated by soft and flexible hydrogels with lower storage modulus [95]. Such hydrogels are selected for tissue engineering applications, where the hydrogel's scaffold provides a suitable environment for cell growth and tissue regeneration.

The storage and loss moduli of a hydrogel significantly affect its mucoadhesive properties [96]. In the context of mucoadhesion, a hydrogel with higher storage modulus promotes better contact and adherence to the mucosal surface, since it has necessary strength and cohesion to prevent detachment and withstand shear forces [97]. A hydrogel with higher loss modulus contributes to improved wetting and spreading on the mucosal surface, which allows an intimate contact of the hydrogel with the mucosal surface [98].

A right balance between the storage and loss moduli is important while selecting a hydrogel for drug delivery and mucoadhesion. Hydrogels with a good balance between the storage and loss modulus exhibit both 1) ability to have an intimate contact with the mucus layer or with biological tissues, 2) sufficient mechanical strength to adhere to the mucus layer or with biological tissues. These two factors are crucial while facilitating drug delivery and absorption.

Table 2 gives a summary of the rheological properties of the hydrogels, which are used for drug delivery and for mucoadhesion, that we reviewed.

 doi:10.20944/preprints202306.0172.v1

Table 2. Details of the rheological properties of the hydrogels considered in this review.

Hydrogel Used	Research Conducted by	Comments by the Research Group on the Hydrogel's Rheological Properties
Native mucus	Wolf et al.	G′>G″
	Hill et al.	G′>G″
Poly vinyl alcohol	Suzuki et al.	G′ and G″ remained a constant up to 50°C and decreased later.
	Park et al.	G′ decreased as the temperature increased.
	Narita et al.	At lower frequencies, G′< G″, and at higher frequencies, G′> G″.
	Lu et al.	At lower frequencies, G″ > G′, and at higher frequencies, G′ >G″
Polyvinyl alcohol with boron	Lin et al.	At lower frequency G′< G″, and at higher frequency the G′> G″.
	Vinod et al.	G′> G″
Guar gum borax	Pan et al.	G′> G″
	Sun et al.	G′> G″
	Sharma et al.	For MIH-1, G′ > G″ For MIH-2 and MIH-3, G″ > G′
Polyglycerol	Lospichl et al.	G′> G″
	Ekinci et al.	G′ < G″
	Kim et al.	G′ > G″
Polyacrylic acid	Bonacucina et al.	G′ > G″
	Baek et al.	G′ > G″
	Schenck et al.	G′> G″
	Vicente et al.	G′ > G″

Table 3. Details of the tribological properties of the hydrogels considered in this review.

Hydrogel Used	Research Conducted by	Comments by the Research Group on the Hydrogel's Tribological Properties
Native mucus	Albers et al.	Measured the work of adhesion needed to move native mucus from the airway duct: • Using the ring method, the values ranged from 130 ± 20 mN/m to 140 ± 30 mN/m. • Using the contact angle method 150 ± 20 mN/m-160±20 mN/m
	King et al.	As the work of adhesion increased, the transportability of the mucus decreased.
Poly vinyl alcohol	Vinod et al.	The lateral force, f_{II}, for sliding = 111 μN.
Polyvinyl alcohol with boron	Cui et al.	The coefficient of friction (COF): • PVA hydrogel, COF = 0.159. • PVA Borax hydrogel, COF = 0.077.
	Vinod et al.	The lateral force, f_{II}, needed to slide the hydrogel drop was around 166 μN.
Guar gum with scleroglucan	Lafforgue et al.	The surface tension of the hydrogel = 71.6 to 89.9 mN/m.
Guar gum borax	Pan et al.	The work of adhesion required to detach the hydrogel from the

 doi:10.20944/preprints202306.0172.v1

		'human skin mimicking surface' was 2.5 KPa.
Polyglycerol	Orafai et al.	Surface energy of the hydrogel = 31.38 mJ/m to 62.41 mJ/m.
	Schenck	Surface tensions were recorded for different weight percentage of polymer in the hydrogel: • 0.025 % - 2.33± 0.12 mN/m • 0.04 % - 71.63± 0.23 mN/m • 0.05 % - 71.77± 0.37 mN/m
	Chau et al.	The coefficient of friction (COF) was recorded based on the pH of the hydrogel: • pH = 0.35, 0 wt % acrylic acid: COF = 0.17±0.01 • pH = 7, 12 wt % acrylic acid: COF= 0.005±0.001
Polyacrylic acid	Ma et al.	The coefficient of friction was recorded based on the pH of the hydrogel • pH = 2: COF= 0.3-0.4

Conclusion

Human mucus mimicking hydrogels are synthetic hydrogels designed to replicate the physical properties of mucus found in human body. These hydrogels typically consist of water swollen polymers and other substances that bind the polymer chains together. One of their key characteristics is the ability to accurately mimic the rheological and tribological behavior of natural human mucus. This unique capability has led to a wide range of applications for these hydrogels, including their use as drug delivery systems and their utility in medical research, particularly in the study of respiratory diseases like cystic fibrosis, asthma, and chronic obstructive pulmonary disease.

In this review, most of the hydrogels examined demonstrated a higher storage modulus than loss modulus, indicating their suitability for drug delivery and mucoadhesive purposes. Furthermore, we conducted direct measurements of the work of adhesion, and lateral forces required to detach and slide PVA Borax hydrogel on a hydrophobic surface that has been silanized with silicon.

References

1. P. Jeffery, D. Gaillard, S. Moret, H. Maison Blanche, Human airway secretory cells during development and in mature airway epithelium, 1992.
2. S. Girod, J.-M. Zahm, C. Plotkowski, G. Beck, E. Puchelle, Role of the physicochemical properties of mucus in the protection of the respiratory epithelium, 1992.
3. M.E.V. Johansson, H. Sjövall, G.C. Hansson, The gastrointestinal mucus system in health and disease, *Nat Rev Gastroenterol Hepatol*. 10, (2013).
4. L.M. Ensign, B.C. Tang, Y.Y. Wang, T.A. Tse, T. Hoen, R. Cone, J. Hanes, Mucus-penetrating nanoparticles for vaginal drug delivery protect against herpes simplex virus, *Sci Transl Med*. 4, (2012).
5. B. Button, R.C. Boucher, Role of mechanical stress in regulating airway surface hydration and mucus clearance rates, *Respir Physiol Neurobiol*. 163, (2008).
6. J.D. Smart, The basics and underlying mechanisms of mucoadhesion, *Adv Drug Deliv Rev*. 57, (2005).
7. J. V. Fahy, B.F. Dickey, Airway Mucus Function and Dysfunction, *New England Journal of Medicine*. 363, (2010).
8. J.Y. Lock, T.L. Carlson, R.L. Carrier, Mucus models to evaluate the diffusion of drugs and particles, *Adv Drug Deliv Rev*. 124, (2018).
9. Bossi R, Methods for collecting and measuring mucus in human, *Methods in Bronchial Mucology*. 13–20, (1988).
10. A. Jeanneret-Grosjean, M. King, M.C. Michoud, H. Liote, R. Amyot, Sampling technique and rheology of human tracheobronchial mucus, *American Review of Respiratory Disease*. 137, (1988).
11. D.F. Proctor, E.F. Aharonson, M.J. Reasor, K.R. Bucklen, A method for collecting normal respiratory mucus, *BULL.PHYSIO-PATH.RESP.* 9, (1973).
12. J.G. Zayas, G.C.W. Man, M. King, Tracheal mucus rheology in patients undergoing diagnostic bronchoscopy. Interrelations with smoking and cancer, *American Review of Respiratory Disease*. 141, (1990).

 doi:10.20944/preprints202306.0172.v1

13. M. King, P.T. Macklem, Rheological properties of microliter quantities of normal mucus, *J Appl Physiol Respir Environ Exerc Physiol*. 42, (1977).
14. D.B. Hill, B. Button, M. Rubinstein, R.C. Boucher, PHYSIOLOGY AND PATHOPHYSIOLOGY OF HUMAN AIRWAYMUCUS, *Physiol Rev*. 102, (2022).
15. H.H. Winter, F. Chambon, Analysis of Linear Viscoelasticity of a Crosslinking Polymer at the Gel Point, *J Rheol (N Y N Y)*. 30, (1986).
16. H.L. Lin, W.H. Liu, K.S. Shen, T.L. Yu, C.H. Cheng, Weak Gel Behaviour of Poly(vinyl alcohol)-Borax Aqueous Solutions, *Journal of Polymer Research*. 10, (2003).
17. H.H. Winter, Can the gel point of a cross-linking polymer be detected by the G′ – G″ crossover?, *Polym Eng Sci*. 27, (1987).
18. J.E. Martin, D. Adolf, J.P. Wilcoxon, Viscoelasticity near the sol-gel transition, *Phys Rev A (Coll Park)*. 39, (1989).
19. A. Izuka, H.H. Winter, T. Hashimoto, Molecular Weight Dependence of Viscoelasticity of Polycaprolactone Critical Gels, *Macromolecules*. 25, (1992).
20. D.P. Wolf, L. Blasco, M.A. Khan, M. Litt, Human cervical mucus. I. Rheologic characteristics, *Fertil Steril*. 28, (1977).
21. D.B. Hill, P.A. Vasquez, J. Mellnik, S.A. McKinley, A. Vose, F. Mu, A.G. Henderson, S.H. Donaldson, N.E. Alexis, R.C. Boucher, M.G. Forest, A biophysical basis for mucus solids concentration as a candidate biomarker for airways disease, *PLoS One*. 9, (2014).
22. A.M. LUCAS, L.C. DOUGLAS, PRINCIPLES UNDERLYING CILIARY ACTIVITY IN THE RESPIRATORY TRACT: II. A COMPARISON OF NASAL CLEARANCE IN MAN, MONKEY AND OTHER MAMMALS, *Archives of Otolaryngology - Head and Neck Surgery*. 20, (1934).
23. G.M. Albers, R.P. Tomkiewicz, M.K. May, O.E. Ramirez, B.K. Rubin, Ring distraction technique for measuring surface tension of sputum: Relationship to sputum clearability, *J Appl Physiol*. 81, (1996).
24. M. King, J.M. Zahm, D. Pierrot, S. Vaquez-Girod, E. Puchelle, The role of mucus gel viscosity, spinnability, and adhesive properties in clearance by simulated cough, *Biorheology*. 26, (1989).
25. M.E. Schrader, Young-Dupre Revisited, *Langmuir*. 11, (1995).
26. Puchelle E, A simple technique for measuring adhesion tension properties of human bronchial secretions, *Eur. Respir. Dis*. 71, S281, (1987).
27. R.S. Pillai, T. Chandra, I.F. Miller, J. Lloyd-Still, D.B. Yeates, Work of adhesion of respiratory tract mucus, in: J Appl Physiol, 1992.
28. G.M. Albers, R.P. Tomkiewicz, M.K. May, O.E. Ramirez, B.K. Rubin, Ring distraction technique for measuring surface tension of sputum: Relationship to sputum clearability, *J Appl Physiol*. 81, (1996).
29. V.I. Lozinsky, E.S. Vainerman, L. v. Domotenko, A.M. Mamtsis, E.F. Titova, E.M. Belavtseva, S. v. Rogozhin, Study of cryostructurization of polymer systems VII. Structure formation under freezing of poly(vinyl alcohol) aqueous solutions, *Colloid Polym Sci*. 264, (1986).
30. M. Watase, K. Nishinari, Thermal and rheological properties of poly(vinyl alcohol) hydrogels prepared by repeated cycles of freezing and thawing, *Die Makromolekulare Chemie*. 189, (1988).
31. G. Paradossi, F. Cavalieri, E. Chiessi, C. Spagnoli, M.K. Cowman, Poly(vinyl alcohol) as versatile biomaterial for potential biomedical applications, in: J Mater Sci Mater Med, 2003.
32. S. Jiang, S. Liu, W. Feng, PVA hydrogel properties for biomedical application, *J Mech Behav Biomed Mater*. 4, (2011).
33. B. Singh, L. Pal, Sterculia crosslinked PVA and PVA-poly(AAm) hydrogel wound dressings for slow drug delivery: Mechanical, mucoadhesive, biocompatible and permeability properties, *J Mech Behav Biomed Mater*. 9, (2012).
34. K.M. Krise, A.A. Hwang, D.M. Sovic, B.H. Milosavljevic, Macro- and microscale rheological properties of poly(vinyl alcohol) aqueous solutions, *Journal of Physical Chemistry B*. 115, (2011).
35. H. Fujita, E. Maekawa, Viscosity behavior of the system polymethyl acrylate and diethyl phthalate over the complete range of composition, *Journal of Physical Chemistry*. 66, (1962).
36. F. Samadi, B.A. Wolf, Y. Guo, A. Zhang, A.D. Schlüter, Branched versus linear polyelectrolytes: Intrinsic viscosities of peripherically charged dendronized poly(methyl methacrylate)s and of their uncharged analogues, *Macromolecules*. 41, (2008).
37. I.E. LăMĂtic, M. Bercea, S. Morariu, Intrinsic viscosity of aqueous polyvinyl alcohol solutions, *Revue Roumaine de Chimie*. 54, (2009).
38. J.S. Park, J.W. Park, E. Ruckenstein, On the viscoelastic properties of poly(vinyl alcohol) and chemically crosslinked poly(vinyl alcohol), *J Appl Polym Sci*. 82, (2001).
39. T. Narita, K. Mayumi, G. Ducouret, P. Hébraud, Viscoelastic properties of poly(vinyl alcohol) hydrogels having permanent and transient cross-links studied by microrheology, classical rheometry, and dynamic light scattering, *Macromolecules*. 46, (2013).
40. R. Tadmor, P. Bahadur, A. Leh, H.E. N'Guessan, R. Jaini, L. Dang, Measurement of lateral adhesion forces at the interface between a liquid drop and a substrate, *Phys Rev Lett*. 103, 266101, (2009).

 doi:10.20944/preprints202306.0172.v1

41. A. Vinod, Y.V. Reddy Bhimavarapu, M. Hananovitz, Y. Stern, S. Gulec, A.K. Jena, S. Yadav, E.J. Gutmark, P.K. Patra, R. Tadmor, Mucus-Inspired Tribology, a Sticky Yet Flowing Hydrogel, *ACS Appl Polym Mater*. (2022).
42. E.A. Kamoun, X. Chen, M.S. Mohy Eldin, E.R.S. Kenawy, Crosslinked poly(vinyl alcohol) hydrogels for wound dressing applications: A review of remarkably blended polymers, *Arabian Journal of Chemistry*. 8, (2015).
43. S. Spoljaric, A. Salminen, N.D. Luong, J. Seppälä, Stable, self-healing hydrogels from nanofibrillated cellulose, poly(vinyl alcohol) and borax via reversible crosslinking, *Eur Polym J*. (2014).
44. B. Lu, F. Lin, X. Jiang, J. Cheng, Q. Lu, J. Song, C. Chen, B. Huang, One-Pot Assembly of Microfibrillated Cellulose Reinforced PVA-Borax Hydrogels with Self-Healing and pH-Responsive Properties, *ACS Sustain Chem Eng*. 5, (2017).
45. L. Cui, J. Chen, C. Yan, D. Xiong, Mechanical and Biotribological Properties of PVA/SB Triple-Network Hydrogel for Biomimetic Artificial Cartilage, *J Bionic Eng*. (2022).
46. A. Theocharidou, I. Mourtzinos, C. Ritzoulis, The role of guar gum on sensory perception, on food function, and on the development of dysphagia supplements – A review, *Food Hydrocolloids for Health*. 2, (2022).
47. A. George, P.A. Shah, P.S. Shrivastav, Natural biodegradable polymers based nano-formulations for drug delivery: A review, *Int J Pharm*. 561, (2019).
48. N. Thombare, U. Jha, S. Mishra, M.Z. Siddiqui, Guar gum as a promising starting material for diverse applications: A review, *Int J Biol Macromol*. 88, (2016).
49. M. Hussain, S. Bakalis, O. Gouseti, T. Zahoor, F.M. Anjum, M. Shahid, Dynamic and shear stress rheological properties of guar galactomannans and its hydrolyzed derivatives, *Int J Biol Macromol*. 72, (2015).
50. T. Coviello, P. Matricardi, F. Alhaique, R. Farra, G. Tesei, S. Fiorentino, F. Asaro, G. Milcovich, M. Grassi, Guar gum/borax hydrogel: Rheological, low field NMR and release characterizations, *Express Polym Lett*. 7, (2013).
51. T. Coviello, F. Alhaique, A. Dorigo, P. Matricardi, M. Grassi, Two galactomannans and scleroglucan as matrices for drug delivery: Preparation and release studies, *European Journal of Pharmaceutics and Biopharmaceutics*. 66, (2007).
52. I. Gliko-Kabir, B. Yagen, A. Penhasi, A. Rubinstein, Low swelling, crosslinked guar and its potential use as colon-specific drug carrier, *Pharm Res*. 15, (1998).
53. N. Dangi, B.S. Yadav, R.B. Yadav, Pasting, rheological, thermal and gel textural properties of pearl millet starch as modified by guar gum and its acid hydrolysate, *Int J Biol Macromol*. 139, (2019).
54. J.M. Zahm, M. King, C. Duvivier, D. Pierrot, S. Girod, E. Puchelle, Role of simulated repetitive coughing in mucus clearance, *European Respiratory Journal*. (1991).
55. D. Quemada, R. Droz, Blood viscoelasticity and thixotropy from stress formation and relaxation measurements: A unified model, *Biorheology*. 20, (1983).
56. O. Lafforgue, N. Bouguerra, S. Poncet, I. Seyssiecq, J. Favier, S. Elkoun, Thermo-physical properties of synthetic mucus for the study of airway clearance, *J Biomed Mater Res A*. 105, 3025–3033, (2017).
57. T.G. Mezger, The Rheology Handbook - For users of rotational and oscillatory rheometers, 2006.
58. S.K. Lai, Y.Y. Wang, D. Wirtz, J. Hanes, Micro- and macrorheology of mucus, *Adv Drug Deliv Rev*. 61, (2009).
59. S. Kesavan, R.K. Prud'homme, Rheology of Guar and HPG Cross-Linked by Borate, *Macromolecules*. 25, (1992).
60. A. Tayal, V.B. Pai, S.A. Khan, Rheology and microstructural changes during enzymatic degradation of a guar-borax hydrogel, *Macromolecules*. 32, (1999).
61. X. Pan, Q. Wang, D. Ning, L. Dai, K. Liu, Y. Ni, L. Chen, L. Huang, Ultraflexible Self-Healing Guar Gum-Glycerol Hydrogel with Injectable, Antifreeze, and Strain-Sensitive Properties, *ACS Biomater Sci Eng*. 4, (2018).
62. C. Sun, Y. Boluk, Rheological behavior and particle suspension capability of guar gum: sodium tetraborate decahydrate gels containing cellulose nanofibrils, *Cellulose*. 23, (2016).
63. R. Bej, R. Haag, Mucus-Inspired Dynamic Hydrogels: Synthesis and Future Perspectives, *J Am Chem Soc*. 144, 20137–20152, (2022).
64. A. Sharma, B. Thongrom, S. Bhatia, B. von Lospichl, A. Addante, S.Y. Graeber, D. Lauster, M.A. Mall, M. Gradzielski, R. Haag, Polyglycerol-Based Mucus-Inspired Hydrogels, *Macromol Rapid Commun*. 42, (2021).
65. S.H. Mahadevegowda, M.C. Stuparu, Thermoresponsive Corannulene, *European J Org Chem*. 2017, (2017).
66. B. von Lospichl, S. Hemmati-Sadeghi, P. Dey, T. Dehne, R. Haag, M. Sittinger, J. Ringe, M. Gradzielski, Injectable hydrogels for treatment of osteoarthritis – A rheological study, *Colloids Surf B Biointerfaces*. 159, (2017).
67. D. Ekinci, A.L. Sisson, A. Lendlein, Polyglycerol-based polymer network films for potential biomedical applications, *J Mater Chem*. 22, (2012).

68. V.N.A. Le, J.W. Lin, Tribological properties of aluminum nanoparticles as additives in an aqueous glycerol solution, *Applied Sciences (Switzerland)*. 7, (2017).
69. H. Orafai, P. Kallinteri, M. Garnett, S. Huggins, G. Hutcheon, C. Pourcain, Novel poly(glycerol-adipate) polymers used for nanoparticle making: A study of surface free energy, *Iranian Journal of Pharmaceutical Research*. 7, (2008).
70. D.H. Kaelble, Dispersion-Polar Surface Tension Properties of Organic Solids, *J Adhes*. 2, (1970).
71. D.Y. Kwok, A.W. Neumann, Contact angle measurement and contact angle interpretation, *Adv Colloid Interface Sci*. 81, (1999).
72. F.M. Fowkes, Determination of interfacial tensions, contact angles, and dispersion forces in surfaces by assuming additivity of intermolecular interactions in surfaces [5], *Journal of Physical Chemistry*. 66, (1962).
73. H. Park, J.R. Robinson, Mechanisms of Mucoadhesion of Poly(acrylic Acid) Hydrogels, *Pharmaceutical Research: An Official Journal of the American Association of Pharmaceutical Scientists*. 4, (1987).
74. H. Arkaban, M. Barani, M.R. Akbarizadeh, N.P.S. Chauhan, S. Jadoun, M.D. Soltani, P. Zarrintaj, Polyacrylic Acid Nanoplatforms: Antimicrobial, Tissue Engineering, and Cancer Theranostic Applications, *Polymers (Basel)*. 14, (2022).
75. N. Ahmad, M.C.I.M. Amin, S.M. Mahali, I. Ismail, V.T.G. Chuang, Biocompatible and mucoadhesive bacterial cellulose-g-poly(acrylic acid) hydrogels for oral protein delivery, *Mol Pharm*. 11, (2014).
76. B.W. Barry, M.C. Meyer, The rheological properties of carbopol gels I. Continuous shear and creep properties of carbopol gels, *Int J Pharm*. 2, (1979).
77. S. Tamburic, D.Q.M. Craig, A comparison of different in vitro methods for measuring mucoadhesive performance, *European Journal of Pharmaceutics and Biopharmaceutics*. 44, (1997).
78. H. Hägerström, M. Paulsson, K. Edsman, Evaluation of mucoadhesion for two polyelectrolyte gels in simulated physiological conditions using a rheological method, *European Journal of Pharmaceutical Sciences*. 9, (2000).
79. R.G. Riley, J.D. Smart, J. Tsibouklis, P.W. Dettmar, F. Hampson, J.A. Davis, G. Kelly, W.R. Wilber, An investigation of mucus/polymer rheological synergism using synthesised and characterised poly(acrylic acid)s, *Int J Pharm*. 217, (2001).
80. J.Y. Kim, J.Y. Song, E.J. Lee, S.K. Park, Rheological properties and microstructures of Carbopol gel network system, *Colloid Polym Sci*. 281, (2003).
81. G. Bonacucina, S. Martelli, G.F. Palmieri, Rheological, mucoadhesive and release properties of Carbopol gels in hydrophilic cosolvents, *Int J Pharm*. 282, (2004).
82. G. Baek, C. Kim, Rheological properties of Carbopol containing nanoparticles, *J Rheol (N Y N Y)*. 55, (2011).
83. D.M. Schenck, J. Fiegel, Tensiometric and Phase Domain Behavior of Lung Surfactant on Mucus-like Viscoelastic Hydrogels, *ACS Appl Mater Interfaces*. 8, (2016).
84. G.H. Koenderink, M. Atakhorrami, F.C. MacKintosh, C.F. Schmidt, High-frequency stress relaxation in semiflexible polymer solutions and networks, *Phys Rev Lett*. 96, (2006).
85. R. Hamed, J. Fiegel, Synthetic tracheal mucus with native rheological and surface tension properties, *J Biomed Mater Res A*. 102, (2014).
86. J. De Vicente, J.R. Stokes, H.A. Spikes, Soft lubrication of model hydrocolloids, in: Food Hydrocoll, 2006.
87. A.L. Chau, P.T. Getty, A.R. Rhode, C.M. Bates, C.J. Hawker, A.A. Pitenis, Superlubricity of pH-responsive hydrogels in extreme environments, *Front Chem*. 10, (2022).
88. Y. Sun, D. Nan, H. Jin, X. Qu, Recent advances of injectable hydrogels for drug delivery and tissue engineering applications, *Polym Test*. 81, (2020).
89. T.R. Hoare, D.S. Kohane, Hydrogels in drug delivery: Progress and challenges, *Polymer (Guildf)*. 49, (2008).
90. C.S. Pereira, A.M. Cunha, R.L. Reis, B. Vázquez, J. San Román, New starch-based thermoplastic hydrogels for use as bone cements or drug-delivery carriers, *J Mater Sci Mater Med*. 9, (1998).
91. J. Li, L. Ma, G. Chen, Z. Zhou, Q. Li, A high water-content and high elastic dual-responsive polyurethane hydrogel for drug delivery, *J Mater Chem B*. 3, (2015).
92. A. Islam, M. Riaz, T. Yasin, Structural and viscoelastic properties of chitosan-based hydrogel and its drug delivery application, *Int J Biol Macromol*. 59, (2013).
93. E. Engleder, C. Honeder, J. Klobasa, M. Wirth, C. Arnoldner, F. Gabor, Preclinical evaluation of thermoreversible triamcinolone acetonide hydrogels for drug delivery to the inner ear, *Int J Pharm*. 471, (2014).
94. K.Y. Lee, D.J. Mooney, Hydrogels for tissue engineering, *Chem Rev*. 101, 1869–1879, (2001).
95. N. Vázquez-Portalatín, C.E. Kilmer, A. Panitch, J.C. Liu, Characterization of Collagen Type i and II Blended Hydrogels for Articular Cartilage Tissue Engineering, *Biomacromolecules*. 17, (2016).
96. F. Madsen, K. Eberth, J.D. Smart, A rheological examination of the mucoadhesive/mucus interaction: The effect of mucoadhesive type and concentration, *Journal of Controlled Release*. 50, (1998).
97. S.A. Mortazavi, J.D. Smart, An investigation into the role of water movement and mucus gel dehydration in mucoadhesion, *Journal of Controlled Release*. 25, (1993).

 doi:10.20944/preprints202306.0172.v1

98. M. Nur, L. Ramchandran, T. Vasiljevic, Tragacanth as an oral peptide and protein delivery carrier: Characterization and mucoadhesion, *Carbohydr Polym*. 143, (2016).